

# Hybrid Data Impedance Tomography with the Complete Electrode Model

Jeppe Bo Andersen

DTU



Kongens Lyngby 2016

Technical University of Denmark  
Department of Applied Mathematics and Computer Science  
Richard Petersens Plads, building 324,  
2800 Kongens Lyngby, Denmark  
Phone +45 4525 3031  
[compute@compute.dtu.dk](mailto:compute@compute.dtu.dk)  
[www.compute.dtu.dk](http://www.compute.dtu.dk)

# Summary (English)

---

We consider the Complete Electrode Model (CEM) as a model for the scenario where one apply currents to electrodes attached at the surface of the body.

We show, using two different approaches, that the forward problem for the CEM has a unique solution. Firstly, by Lax-Milgram Theorem, we identify the forward problem by the variational formulation (2.1). Secondly, via a minimization approach, by associating the forward problem with the functional  $F_\sigma$  (2.52).

Using the magnitude of the current density, we show non-uniqueness of the inverse problem of finding the conductivity. We characterize this non-uniqueness and state when reconstruction of the conductivity is possible.

Numerical experiments of both problems show that errors occur at discontinuities of the conductivity and around the electrodes.



# Summary (Danish)

---

Vi benytter den fuldstændige elektrode model (CEM) til at betragte scenariet, hvor strøm sendes gennem kroppen, via et antal elektroder fastspændt på denne.

Ved to forskellige fremgangsmåder vises det, at den partielle differentiaalligning for CEM har en entydig løsning. Først relateres PDE'en til formulering (2.1) og derefter vises entydighed ved brug af Lax-Milgram's sætning. Dernæst identificeres PDE'en med minimeringen af funktionalet (2.52).

Vi viser, ved hjælp af kendskab til strømtætheden i kroppen, at det inverse problem, at finde ledningsevnen, ikke har en entydig løsning. Vi karakterisere dette og viser hvordan man kan rekonstruere ledningsevnen ved kendskab til spændingen på randen.

Numeriske eksperimenter af begge problemer viser, at fejlene opstår ved diskontinuerte områder af ledningsevnen og omkring elektroderne.



# Preface

---

This thesis was prepared at DTU Compute in fulfilment of the requirements for acquiring an M.Sc. in Engineering.

The thesis deals with problems regarding Electrical Impedance Tomography (EIT) and Current Density Impedance Imaging (CDII).

Lyngby, 24-January-2016

Jeppe Bo Andersen





# Acknowledgements

---

I would like to thank my advisers Kim Knudsen and Kaloyan Marinov, both DTU Compute, Technical University of Denmark, for the guidance through the past five months.

They have helped me with all from project definition to understanding complex theory and doing numerical computations. This have been a very big help for me and I sincerely appreciate it.

Last I would like to thank Stratos Stambouli, DTU Compute, for helping with the interpretation of the convergence orders for solutions of the forward problem.



# Contents

---

Summary (English)	i
Summary (Danish)	iii
Preface	v
Acknowledgements	vii
<b>1 Introduction</b>	<b>1</b>
<b>2 Electrical Impedance Tomography: The Forward Problem</b>	<b>5</b>
2.1 A variational formulation of the CEM . . . . .	6
2.2 Unique solvability of the forward problem via Lax-Milgram . . . . .	9
2.3 Unique solvability of the forward problem via minimization . . . . .	18
<b>3 Current Density Impedance Imaging</b>	<b>27</b>
3.1 Defining a minimal gradient problem . . . . .	28
3.2 Characterization of non-uniqueness . . . . .	29
<b>4 Experiments of the forward problem</b>	<b>35</b>
4.1 Implementing the CEM . . . . .	36
4.2 Experiments with constant conductivity . . . . .	38
4.3 Experiments with smooth conductivity . . . . .	39
4.4 Experiments with piecewise constant conductivity . . . . .	41
4.5 Conclusion on experiments . . . . .	43
<b>5 Reconstructing conductivity</b>	<b>45</b>
5.1 Algorithm for reconstruction . . . . .	45
5.2 Generating $\phi$ . . . . .	48

---

5.3	Reconstruction with smooth conductivity . . . . .	49
5.4	Reconstruction with piecewise constant conductivity . . . . .	53
<b>6</b>	<b>Conclusion and Perspective</b>	<b>61</b>
<b>A</b>	<b>Definitions, theorems, etc.</b>	<b>63</b>
A.1	Notes on traces, $H^{1/2}$ and $H^{-1/2}$ . . . . .	63
A.2	Theorems, propositions, etc. . . . .	64
<b>B</b>	<b>Pieces of code</b>	<b>69</b>
B.1	Defining mesh, electrodes, function space etc. . . . .	69
B.2	Construction of conductivity . . . . .	71
B.3	Solving the forward problem . . . . .	72
B.4	Calculating errors . . . . .	74
B.5	Algorithm for the inverse problem . . . . .	74
<b>C</b>	<b>Original Project Plan</b>	<b>77</b>
C.1	Original Project Plan . . . . .	77
C.1.1	Learning objectives . . . . .	78
C.1.2	Goals . . . . .	78
	<b>Bibliography</b>	<b>81</b>

# CHAPTER 1

## Introduction

---

We will in this thesis consider problems appearing in Electrical Impedance Tomography (EIT) and Current Density Impedance Imaging (CDII).

Using EIT imaging technique one place a number of electrodes on the surface of the skin. Through each electrode,  $e_k$ , we apply a current,  $I_k$ , which results in a voltage,  $u$ , throughout the body and a constant voltage,  $U_k$ , on each electrode. From a medical aspect it is important to find the conductivity,  $\sigma$ , inside the body, since the conductivity of different tissues varies significantly from each other.

As a model for the given scenario we use the Complete Electrode Model (CEM) for EIT presented in [SCI92]. Given a current pattern  $\{I_k\}_{k=1}^N \subset \mathbb{R}$  with  $\sum_{k=1}^N I_k = 0$ , we seek a pair  $(u, U) \in \mathcal{H} := H^1(\Omega) \times \mathbb{C}^N$ , s.t.  $(u, U)$  solves

the boundary-value problem:

$$\nabla \cdot \sigma \nabla u = 0 \quad \text{in } \Omega \quad (1.1)$$

$$u + z_k \sigma \frac{\partial u}{\partial n} = U_k \quad \text{on } e_k \text{ for all } k = 1, \dots, N \quad (1.2)$$

$$\sigma \frac{\partial u}{\partial n} = 0 \quad \text{on } \partial\Omega \setminus \bigcup_{k=1}^N e_k \quad (1.3)$$

$$\int_{e_k} \sigma \frac{\partial u}{\partial n} ds = I_k \quad \text{for all } k = 1, \dots, N \quad (1.4)$$

Here the impedances  $\{z_k\}_{k=1}^N$  are known constants and  $n$  are the out warded unit normal. The boundary value problem (1.1)-(1.4) will from now on be referred to as the forward problem.

We will show that the forward problem has a unique solution provided an extra condition on  $U$  given by  $\sum_{k=1}^N U_k = 0$ . Uniqueness is shown via two different approaches. Firstly we will show that there is a 1-to-1-correspondence between the forward problem and the variational formulation

$$B((u, U), (v, V)) = \sum_{k=1}^N I_k \bar{V}_k, \quad \text{for all } (v, V) \in \mathcal{H}, \quad (1.5)$$

where  $B$  is defined by

$$B((u, U), (v, V)) = \int_{\Omega} \sigma \nabla u \cdot \nabla \bar{v} dx + \sum_{k=1}^N \frac{1}{z_k} \int_{e_k} (u - U_k)(\bar{v} - \bar{V}_k) ds. \quad (1.6)$$

Showing that  $B$  satisfies the assumptions of the Lax-Milgram Theorem establishes unique solvability of the forward problem.

Secondly we prove uniqueness through a minimization problem associating the forward problem with the functional

$$F_{\sigma}(u, U) = \frac{1}{2} \int_{\Omega} \sigma |\nabla u|^2 dx + \frac{1}{2} \sum_{k=1}^N \int_{e_k} \frac{1}{z_k} (u - U_k)^2 ds - \sum_{k=1}^N I_k U_k. \quad (1.7)$$

Next we consider the inverse problem of finding the conductivity. We state and prove non-uniqueness of this and using the magnitude of the current density we characterize the non-uniqueness.

To show non-uniqueness of the inverse problem we consider the functional:

$$G_a(v, V) = \int_{\Omega} a |\nabla v| dx + \sum_{k=1}^N \int_{e_k} \frac{1}{2z_k} (v - V_k)^2 ds - \sum_{k=1}^N I_k V_k. \quad (1.8)$$

Here  $a$  denotes the magnitude of the current density  $a := \sigma |\nabla u|$ . We show that a solution to the forward problem, with conductivity  $\sigma$ , is a minimizer of  $G_a$ . Next we show and characterize the non-uniqueness by showing, that if two pairs  $(\sigma, u)$  and  $(\tilde{\sigma}, \tilde{u})$  satisfies  $\sigma |\nabla u| = \tilde{\sigma} |\nabla \tilde{u}|$ , they both minimize  $G_a$  and there exists a function  $\phi$  relating these pairs. This relation also makes it possible to solve the inverse problem, provided knowledge of the voltage on some part of the boundary, including all the electrodes.

The main goal of the thesis is two investigate the non-uniqueness of the inverse problem through theory and numerical experiments. We wish to identify the errors and how they occur, when reconstructing the conductivity. Finally we try decreasing these errors.

The structure of the thesis is as follows: In Chapter 2 we study the forward problem. Firstly, in Section 2.1-2.2, by identifying a variational formulation and showing uniqueness via Lax-Milgram, secondly, in Section 2.3, by considering the minimization of  $F_{\sigma}$  and proving the existence of a unique minimizer. In Chapter 3 we study the inverse problem by associating a solution with a minimal gradient problem (Section 3.1) and next, Section 3.2, characterizing the non-uniqueness of the solutions and which information is needed for doing the reconstruction. In Chapter 4 we do numerical experiments of the forward problem, with different choices of conductivity and electrodes. We investigate the convergence rates with respect to the mesh size and interpret the errors. In Chapter 5 we do numerical experiments of the inverse problem. First we describe an algorithm to find a pair  $(\sigma, u)$  depending on the known magnitude of the current density. Secondly we show how to generate the function relating different solutions of the inverse problem. Finally we reconstruct the conductivity in various scenarios and interpret the errors. In Chapter 6 we conclude on the results and put it into perspective.

In Appendix A are some extra notes on spaces, theorems, definitions, etc. used in the thesis. In Appendix B are pieces of the code and comments on these. In Appendix C the original project plan can be found.





# Electrical Impedance Tomography: The Forward Problem

---

In this chapter we consider the forward problem in EIT with complete electrode boundary conditions. The mathematical framework for this is the so-called Complete Electrode Model ((1.1)-(1.4)).

More specifically, consider a domain  $\Omega$  with  $N$  electrodes attached to  $\partial\Omega$ . Assume then that the size, location and contact impedance,  $z_k$ , of each electrode is known. The main goal of this chapter is to prove that, if one injects any admissible current pattern,  $\{I_k\}_{k=1}^N$  with  $\sum_{k=1}^N I_k = 0$ , through the electrodes, then one can uniquely determine the voltage,  $u$ , inside  $\Omega$  as well as the voltage,  $U_k$ , on each electrode. Here the unique determination is in the space  $\mathcal{H} := H^1(\Omega) \times \mathbb{C}^N$ .

In general we will make the following assumptions to the first two sections (2.2 and 2.3) of this chapter: We assume the domain  $\Omega$  is bounded in  $\mathbb{R}^n$ ,  $n = 2, 3$ , with smooth boundary  $\partial\Omega$ . The  $e_k$ 's are open and connected subsets of  $\partial\Omega$  with mutually disjoint closures. We let the conductivity,  $\sigma$ , be a complex-valued function and continuous differentiable in  $\Omega$  up to the boundary, i.e. there exists a neighbourhood  $\mathcal{N}_{\partial\Omega}$  of  $\partial\Omega$ , s.t.  $\sigma \in C^1(\bar{\Omega} \cap \mathcal{N}_{\partial\Omega})$ . Furthermore assume there exists real constants  $\sigma_0$  and  $\sigma_1$ , s.t.  $|\sigma| \leq \sigma_1$  and  $Re(\sigma) \geq \sigma_0$ . For the

impedances we assume there exists a real constant  $Z$  such that  $\operatorname{Re}(z_k) > Z$  for all  $k = 1, \dots, N$ .

## 2.1 A variational formulation of the CEM

In this section we will establish a variational formulation of the forward problem.

First notice that the boundary conditions of the forward problem requires restriction of  $u$  and  $\sigma \frac{\partial u}{\partial n}$  to the boundary  $\partial\Omega$ . This is carried out in Appendix A, section A.1. Here we see that if  $u \in H^1(\Omega)$ , then  $u \in H^{1/2}(\partial\Omega)$  and  $\sigma \frac{\partial u}{\partial n} \in H^{-1/2}(\partial\Omega)$ . The definitions of these spaces are also found in Appendix A.

**PROPOSITION 2.1** *Let  $(u, U) \in \mathcal{H}$ . Then  $(u, U)$  is a weak solution of the forward the problem if and only if*

$$B((u, U), (v, V)) = \sum_{k=1}^N I_k \bar{V}_k, \quad \text{for all } (v, V) \in \mathcal{H} \quad (2.1)$$

Here  $B$  is defined as

$$B((u, U), (v, V)) = \int_{\Omega} \sigma \nabla u \cdot \nabla \bar{v} \, dx + \sum_{k=1}^N \frac{1}{z_k} \int_{e_k} (u - U_k)(\bar{v} - \bar{V}_k) \, ds. \quad (2.2)$$

PROOF. 1. First we prove that, if  $(u, U)$  solves the forward problem it also satisfies (2.1).

Using partial integration, (A.4), and the fact that  $\nabla \cdot \sigma \nabla u = 0$  we have

$$\int_{\partial\Omega} \sigma \frac{\partial u}{\partial n} \bar{v} \, ds - \int_{\Omega} \sigma \nabla u \cdot \nabla \bar{v} \, dx = 0 \quad \forall v \in H^1(\Omega). \quad (2.3)$$

Rewriting (1.2) we have

$$\sigma \frac{\partial u}{\partial n} = \frac{1}{z_k} (U_k - u) \quad \text{on } e_k \text{ for all } k = 1, \dots, N \quad (2.4)$$

and combining with (1.3)

$$\sigma \frac{\partial u}{\partial n} = \sum_{k=1}^N \frac{1}{z_k} (U_k - u) \chi_{e_k}. \quad (2.5)$$

Since  $u \in L^2(\partial\Omega)$  and  $\chi_{e_k}$  is bounded for any  $k$ , the right hand side of (2.5) are in  $L^2(\partial\Omega)$ . Thus is  $\sigma \frac{\partial u}{\partial n} \in L^2(\partial\Omega)$ . Hence, the first integral of (2.3) is well-defined.

Therefore

$$\int_{\partial\Omega} \sigma \frac{\partial u}{\partial n} \bar{v} ds = \sum_{k=1}^N \frac{1}{z_k} \int_{\partial\Omega} (U_k - u) \chi_{e_k} \bar{v} ds = - \sum_{k=1}^N \frac{1}{z_k} \int_{e_k} (u - U_k) \bar{v} ds, \quad (2.6)$$

which, when inserted in (2.3), gives

$$\sum_{k=1}^N \frac{1}{z_k} \int_{e_k} (u - U_k) \bar{v} ds + \int_{\Omega} \sigma \nabla u \cdot \nabla \bar{v} dx = 0. \quad (2.7)$$

Now if we subtract  $U_k$  from both sides of (1.2) and integrate over  $e_k$  we get

$$\int_{e_k} (u - U_k) ds + z_k \int_{e_k} \sigma \frac{\partial u}{\partial n} ds = 0. \quad (2.8)$$

Using (1.4) in the last equality and multiplying by the constant  $\frac{\bar{V}_k}{z_k}$ , where  $V_k \in \mathbb{C}$  is arbitrary, gives

$$\frac{1}{z_k} \int_{e_k} (u - U_k) \bar{V}_k ds + I_k \bar{V}_k = 0, \quad \text{for all } k = 1, \dots, N. \quad (2.9)$$

Next we sum over  $k$  and get

$$\sum_{k=1}^N \frac{1}{z_k} \int_{e_k} (u - U_k) \bar{V}_k ds + \sum_{k=1}^N I_k \bar{V}_k = 0. \quad (2.10)$$

Combining (2.7) and (2.10) we have

$$\sum_{k=1}^N \frac{1}{z_k} \int_{e_k} (u - U_k) \bar{V}_k ds + \sum_{k=1}^N I_k \bar{V}_k = \sum_{k=1}^N \frac{1}{z_k} \int_{e_k} (u - U_k) \bar{v} ds + \int_{\Omega} \sigma \nabla u \cdot \nabla \bar{v} dx. \quad (2.11)$$

Thus

$$\int_{\Omega} \sigma \nabla u \cdot \nabla \bar{v} dx + \sum_{k=1}^N \frac{1}{z_k} \int_{e_k} (u - U_k) (\bar{v} - \bar{V}_k) ds = \sum_{k=1}^N I_k \bar{V}_k, \quad (2.12)$$

for any  $v \in H^1(\Omega)$ . And since the  $V_k$ 's were chosen arbitrary, the above holds for all  $(v, V) \in \mathcal{H}$ , i.e. (2.1) is satisfied.

2. Next, we assume that  $(u, U)$  is a solution to (2.1) for all  $(v, V) \in \mathcal{V}$  and show that  $(u, U)$  is also a solution to the forward problem. By  $(u, U)$  solving (2.1)

for any  $(v, V) \in \mathcal{H}$ , we can choose  $v$  s.t.  $v \in C^\infty(\bar{\Omega})$ ,  $\text{supp}(v) \subset \Omega$ , and  $V = 0$ . This gives us

$$\sum_{k=1}^N I_k \bar{V}_k = 0 \quad (2.13)$$

$$\int_{e_k} (u - U_k)(v - V_k) ds = 0, \quad \text{for all } k = 1, \dots, N, \quad (2.14)$$

since  $v$  is zero on  $\partial\Omega$  and therefore also on  $e_k$ . So by (2.1)

$$\int_{\Omega} \sigma \nabla u \cdot \nabla \bar{v} dx = 0. \quad (2.15)$$

Using (A.4)

$$\int_{\Omega} \nabla \cdot (\sigma \nabla u) \bar{v} dx = 0 \quad \text{for all } v \in C_c^\infty(\bar{\Omega}), \quad (2.16)$$

hence  $\nabla \cdot \sigma \nabla u = 0$  in weak sense. Now choose  $v \in H^1(\Omega)$  arbitrary and  $V = 0$ . Then (A.4) implies

$$\int_{\Omega} \sigma \nabla u \cdot \nabla \bar{v} dx = \int_{\partial\Omega} \sigma \frac{\partial u}{\partial n} \bar{v} ds \quad \text{for all } v \in H^1(\Omega). \quad (2.17)$$

Using this we obtain:

$$\begin{aligned} \int_{\partial\Omega} \sigma \frac{\partial u}{\partial n} \bar{v} ds + \sum_{k=1}^N \frac{1}{z_k} \int_{e_k} (u - U_k) \bar{v} ds \\ = \int_{\partial\Omega} \left( \sigma \frac{\partial u}{\partial n} + \sum_{k=1}^N \frac{1}{z_k} (u - U_k) \chi_{e_k} \right) \bar{v} ds = 0. \end{aligned} \quad (2.18)$$

Since  $v \in L^2(\partial\Omega)$ , (2.18) implies:

$$\sigma \frac{\partial u}{\partial n} + \sum_{k=1}^N \frac{1}{z_k} (u - U_k) \chi_{e_k} = 0 \quad \text{in } L^2(\partial\Omega). \quad (2.19)$$

Therefore:

$$\sigma \frac{\partial u}{\partial n} = - \sum_{k=1}^N \frac{1}{z_k} (u - U_k) \chi_{e_k}, \quad (2.20)$$

so  $(u, U)$  satisfies (1.2) and (1.3). Let us again choose  $v$  with support in  $\Omega$ , but now let  $V \neq 0$ . Then we can write  $B$  as:

$$\begin{aligned} B((u, U), (v, V)) = \int_{\Omega} \sigma \nabla u \cdot \nabla \bar{v} dx + \sum_{k=1}^N \frac{1}{z_k} \int_{e_k} (u - U_k) \bar{v} ds \\ - \sum_{k=1}^N \frac{1}{z_k} \int_{e_k} (u - U_k) \bar{V}_k ds. \end{aligned} \quad (2.21)$$

By the choice of  $v$  and (2.15), this reduces to:

$$B((u, U), (v, V)) = - \sum_{k=1}^N \frac{1}{z_k} \int_{e_k} (u - U_k) \overline{V_k} ds \quad \text{for any } V \neq 0. \quad (2.22)$$

Choosing  $V$  s.t.  $V_j = 1$  and  $V_k = 0$  for  $k \neq j$ , (2.22) becomes

$$B((u, U), (v, V)) = \frac{1}{z_j} \int_{e_j} (U_j - u) ds. \quad (2.23)$$

By (2.1) and the choice of  $V$  this gives

$$\frac{1}{z_j} \int_{e_j} (U_j - u) ds = I_j. \quad (2.24)$$

Finally, since  $(u, U)$  satisfies (1.2):

$$\int_{e_j} \sigma \frac{\partial u}{\partial n} ds = \frac{1}{z_j} \int_{e_j} (U_j - u) ds = I_j. \quad (2.25)$$

This can be done for all  $j = 1, \dots, N$ , thus  $(u, U)$  satisfies (1.4).  $\square$

We have now established the appropriate variational formulation of the forward problem in EIT with complete-electrode boundary conditions. From now on we will therefore consider the forward problem and variational formulation as the same.

## 2.2 Unique solvability of the forward problem via Lax-Milgram

Thanks to Proposition 2.1 from the previous section, establishing unique solvability of the forward problem, is equivalent to establishing unique solvability of the variational problem (2.1). We will carry out the latter task by means of the Lax-Milgram Theorem in the space  $\mathcal{V} = \mathcal{H}/\mathbb{C}$  equipped with the norm:

$$\|(u, U)\|_{\mathcal{V}} = \inf_{c \in \mathbb{C}} (\|u - c\|_{H^1(\Omega)}^2 + \|U - c_N\|_{\mathbb{C}^N}^2)^{1/2}. \quad (2.26)$$

where  $c_N = (c, \dots, c) \in \mathbb{C}^N$ .

The meaning of the space  $\mathcal{V}$  is as follows: Two elements  $(u, U)$  and  $(\tilde{u}, \tilde{U})$  in  $\mathcal{H}$  are considered equivalent in  $\mathcal{V}$  if and only if  $\exists c \in \mathbb{C}$  s.t.  $(u, U) = (\tilde{u} + c, \tilde{U} + c_N)$  in  $\mathcal{H}$ .

**THEOREM 2.2 (Lax-Milgram)** *If  $H$  is a Hilbert-space with norm  $\|\cdot\|$  and  $B$  is a complex-valued functional on  $H \times H$ , which satisfies:*

(i)  $B$  is sesquilinear:

$$\begin{aligned} B(c_1 u_1 + c_2 u_2, v) &= c_1 B(u_1, v) + c_2 B(u_2, v) \\ B(u, c_1 v_1 + c_2 v_2) &= \bar{c}_1 B(u, v_1) + \bar{c}_2 B(u, v_2). \end{aligned}$$

(ii)  $B$  is bounded, i.e.  $\exists c > 0$  s.t.  $|B(u, v)| \leq c\|u\|\|v\|$  for all  $u, v \in H$ .

(iii)  $B$  is coercive, i.e.  $\exists d > 0$  s.t.  $|B(u, u)| \geq d\|u\|^2$  for all  $u \in H$ .

Then for any anti-linear, continuous functional  $f : H \rightarrow \mathbb{C}$ , there exists a unique  $u \in H$  s.t.

$$B(u, v) = f(v), \quad \forall v \in H.$$

The proof of this is carried out in [DL88].

It is quite hard to show boundedness and coercivity of  $B$  on  $\mathcal{V}$  equipped with the norm (2.26). Fortunately, if we introduce another norm as follows:

$$\|(u, U)\|_* = \left( \|\nabla u\|_{L^2(\Omega)}^2 + \sum_{k=1}^N \int_{e_k} |u(x) - U_k|^2 ds \right)^{1/2}, \quad (2.27)$$

we will be able to show equivalence between  $\|\cdot\|_{\mathcal{V}}$  and  $\|\cdot\|_*$  on  $\mathcal{V}$ . Then we will be left to show that  $B$  satisfies the three assumptions of the Lax-Milgram Theorem on  $(\mathcal{V}, \|\cdot\|_*)$ .

**LEMMA 2.3** *The two norms (2.26) and (2.27) are equivalent on  $\mathcal{V}$ , i.e. there exists real constants  $a$  and  $b$ ,  $a < b$ , s.t. for all  $(u, U) \in \mathcal{V}$  the following holds:*

$$a\|(u, U)\|_* \leq \|(u, U)\|_{\mathcal{V}} \leq b\|(u, U)\|_*. \quad (2.28)$$

**PROOF.** We start by showing the first inequality. Let  $(u, U) \in \mathcal{V}$  and  $\epsilon > 0$  be arbitrary. Then, by the definition (2.26), there exists some  $c \in \mathbb{R}$  s.t.

$$\|u - c\|_{H^1(\Omega)}^2 + \|U - c_N\|_{\mathbb{C}^N}^2 \leq \|(u, U)\|_{\mathcal{V}}^2 + \epsilon. \quad (2.29)$$

So

$$\begin{aligned}
\|(u, U)\|_*^2 &= \|(u - c, U - c_N)\|_*^2 \\
&= \|\nabla(u - c)\|_{L^2(\Omega)}^2 + \sum_{k=1}^N \int_{e_k} |u(x) - c - (U_k - c)|^2 ds \\
&\leq \|\nabla(u - c)\|_{L^2(\Omega)}^2 + \sum_{k=1}^N \int_{e_k} (|u - c|^2 + |U_k - c|^2 + 2|u - c||U_k - c|) ds \\
&\leq \|\nabla(u - c)\|_{L^2(\Omega)}^2 + 2 \sum_{k=1}^N \int_{e_k} |u - c|^2 ds + 2 \sum_{k=1}^N \int_{e_k} |U_k - c|^2 ds,
\end{aligned}$$

where the last inequality comes by

$$|(u - c) - (U_k - c)|^2 \geq 0 \Leftrightarrow |u - c|^2 + |U_k - c|^2 \geq 2|(u - c)(U_k - c)|. \quad (2.30)$$

Using that  $\bigcup_{k=1}^N e_k \subset \partial\Omega$ , the first sum can be bounded as follows:

$$\begin{aligned}
\sum_{k=1}^N \int_{e_k} |u - c|^2 ds &\leq \int_{\partial\Omega} |u - c|^2 ds = \|u - c\|_{L^2(\partial\Omega)}^2 \\
&\leq C \cdot \|u - c\|_{H^{1/2}(\partial\Omega)}^2 \leq C \cdot \|u - c\|_{H^1(\Omega)}^2,
\end{aligned}$$

for some  $C > 0$ . The second-to-last inequality follows from the continuous embedding  $H^{1/2}(\partial\Omega) \subset L^2(\partial\Omega)$  and the last inequality follows by (A.3).

The second sum can be bounded by:

$$\sum_{k=1}^N \int_{e_k} |U_k - c|^2 ds \leq \max |e_k| \cdot \sum_{k=1}^N |U_k - c|^2 = D \cdot \|U - c_N\|_{\mathbb{C}^N}^2, \quad (2.31)$$

with  $D = \max |e_k|$ . Since  $\|\nabla(u - c)\|_{L^2(\Omega)} \leq \|\nabla(u - c)\|_{H^1(\Omega)}$ , we have now shown that there exists an  $a > 0$ , depending only on  $\Omega$  and the electrodes, s.t.

$$\|(u, U)\|_*^2 \leq a(\|u - c\|_{H^1(\Omega)}^2 + \|U - c_N\|_{\mathbb{C}^N}^2). \quad (2.32)$$

In view of this and (2.29), we deduce that  $\|(u, U)\|_*^2 \leq a(\|(u, U)\|_{\mathcal{V}}^2 + \epsilon)$  for any  $\epsilon > 0$ , which establishes the first inequality of (2.28).

We will show the second inequality by contradiction. So assume that there exists no such  $b$  satisfying the second inequality of (2.28). Then we can choose a sequence  $\{(u^m, U^m)\}_{m=1}^\infty$  in  $\mathcal{V}$  s.t.

$$\|(u^m, U^m)\|_{\mathcal{V}} = 1 \text{ and } \|(u^m, U^m)\|_* < \frac{1}{m} \text{ for all } m. \quad (2.33)$$

By definition of  $\mathcal{V}$  we may choose complex constants  $\{c^m\}_{m=1}^\infty$  s.t. the sequence  $\{(v^m, V^m)\}_{m=1}^\infty$ , given by  $(v^m, V^m) = (u^m - c^m, U^m - c_N^m)$ , satisfies:

$$1 \leq \|v^m\|_{H^1(\Omega)}^2 + \|V^m\|_{\mathbb{C}^N}^2 < 1 + \frac{1}{m} \text{ for all } m. \quad (2.34)$$

The first inequality of the above comes directly from the definition of the norm  $\|\cdot\|_{\mathcal{V}}$ :

$$\begin{aligned} 1 = \|(u^m, U^m)\|_{\mathcal{V}}^2 &= \inf_{c \in \mathbb{C}} (\|u^m - c\|_{H^1(\Omega)}^2 + \|U^m - c_N\|_{\mathbb{C}^N}^2) \\ &\leq \|u^m - c^m\|_{H^1(\Omega)}^2 + \|U^m - c_N^m\|_{\mathbb{C}^N}^2. \end{aligned}$$

By  $H^1(\Omega)$  being compactly embedded in  $L^2(\Omega)$  we know  $\{v^m\}_{m=1}^\infty$  has a convergent subsequence  $\{v^{m_j}\}_{j=1}^\infty$  in  $L^2(\Omega)$ , i.e. there exists a  $v \in L^2(\Omega)$  s.t.  $v^{m_j} \rightarrow v$  as  $j \rightarrow \infty$ .

On the other hand, since  $\nabla v^{m_j} = \nabla u^{m_j}$  we have that

$$\|\nabla v^{m_j}\|_{L^2(\Omega)}^2 \leq \|(u^{m_j}, U^{m_j})\|_* < \frac{1}{m_j}. \quad (2.35)$$

Therefore  $\{v^{m_j}\}_{m=1}^\infty$  must be a Cauchy sequence in  $H^1(\Omega)$  since

$$\|v^{m_j} - v^{m_i}\|_{H^1(\Omega)} \leq \|v^{m_j} - v^{m_i}\|_{L^2(\Omega)} + \|\nabla v^{m_j}\|_{L^2(\Omega)} + \|\nabla v^{m_i}\|_{L^2(\Omega)} \rightarrow 0 \quad (2.36)$$

as  $i, j \rightarrow \infty$ , where the convergence come by  $v^{m_j}$  converging in  $L^2(\Omega)$ . Being a Cauchy sequence it also converges to some  $v$  satisfying  $\nabla v = 0$ , i.e.  $v \equiv K \in \mathbb{C}$ .

We finally have that

$$\begin{aligned} \frac{1}{m_j} &> \int_{e_k} |u^{m_j} - U_k^{m_j}|^2 ds = \int_{e_k} |v^{m_j} - K - (V_k^{m_j} - K)|^2 ds \\ &= \int_{e_k} |v^{m_j} - K|^2 ds + \int_{e_k} |V_k^{m_j} - K|^2 ds - 2|\overline{V_k^{m_j}} - \overline{K}| \cdot \int_{e_k} |v^{m_j} - K| ds \\ &\geq |e_k| |V_k^{m_j} - K|^2 - 2|V_k^{m_j} - K| \cdot \int_{e_k} |v^{m_j} - K| ds. \end{aligned}$$

So we can write:

$$\begin{aligned} |e_k| |V_k^{m_j} - K|^2 &< \frac{1}{m_j} + 2|V_k^{m_j} - K| \int_{e_k} |v^{m_j} - K| ds \\ &\leq \frac{1}{m_j} + 2(|V_k^{m_j}| + |K|) \int_{e_k} |v^{m_j} - K| ds \\ &\leq \frac{1}{m_j} + 2 \left(1 + \frac{1}{m_j} + |K|\right) |e_k|^{1/2} \|v^{m_j} - K\|_{L^2(\partial\Omega)} \\ &\leq \frac{1}{m_j} + 2C \left(1 + \frac{1}{m_j} + |K|\right) |e_k|^{1/2} \|v^{m_j} - K\|_{H^1(\Omega)}. \end{aligned}$$



The third inequality follows from  $|V_k^{m_j}| \leq \|V^{m_j}\|_{\mathbb{C}^N}^2 < 1 + \frac{1}{m_j}$  and from applying the Cauchy-Schwarz inequality to  $\int_{e_k} |v^{m_j} - K| ds = \int_{\partial\Omega} |v^{m_j} - K| \chi_{e_k} ds$ . The last inequality follows from the continuous embedding  $H^{1/2}(\partial\Omega) \subset L^2(\partial\Omega)$  and (A.3).

Finally, since  $v^{m_j}$  converges to  $K$  in  $H^1(\Omega)$ , the preceding estimate enables us to conclude that  $V_k^{m_j}$  converges to  $K$ , for all  $k = 1, \dots, N$ . Thus we have:

$$1 = \|(u^{m_j}, U^{m_j})\|_{\mathcal{V}}^2 \leq \|v^{m_j} - K\|_{H^1(\Omega)}^2 + \|V^{m_j} - K\|_{\mathbb{C}^N}^2 \rightarrow 0. \quad (2.37)$$

This is a contradiction and therefore we conclude that there exists a  $b$  s.t. the second inequality of (2.28) holds true.  $\square$

Since we now know that the norms (2.26) and (2.27) are equivalent on  $\mathcal{V}$ , showing  $B$  satisfies the assumptions of Lax-Milgram on  $(\mathcal{V}, \|\cdot\|_{\mathcal{V}})$  reduces to show it on  $(\mathcal{V}, \|\cdot\|_*)$ . This is carried out in the next Proposition.

**PROPOSITION 2.4** *Under the assumptions of  $\Omega$ ,  $\sigma$  and  $z_k$  given in the beginning of the chapter, the form  $B$  defined in (2.2) is sesquilinear, bounded and coercive on  $(\mathcal{V}, \|\cdot\|_*)$ .*

**PROOF.** (i) First we show that  $B$  is sesquilinear. Given  $(u_1, U_1)$ ,  $(u_2, U_2)$  and  $(v, V)$  in  $\mathcal{V}$  and complex constants  $c_1$  and  $c_2$ :

$$\begin{aligned} B(c_1(u_1, U_1) + c_2(u_2, U_2), (v, V)) &= \int_{\Omega} \sigma \nabla(c_1 u_1 + c_2 u_2) \cdot \nabla \bar{v} dx \\ &\quad + \sum_{k=1}^N \frac{1}{z_k} \int_{e_k} ((c_1 u_1 + c_2 u_2) - (c_1 U_{1,k} + c_2 U_{2,k})) (\bar{v} - \bar{V}_k) ds \\ &= \int_{\Omega} \sigma \nabla(c_1 u_1) \cdot \nabla \bar{v} + \sigma \nabla(c_2 u_2) \cdot \nabla \bar{v} dx \\ &\quad + \sum_{k=1}^N \frac{1}{z_k} \int_{e_k} c_1 (u_1 - U_{1,k}) (\bar{v} - \bar{V}_k) + c_2 (u_2 - U_{2,k}) (\bar{v} - \bar{V}_k) ds \\ &= c_1 \left( \int_{\Omega} \sigma \nabla u_1 \cdot \nabla \bar{v} dx + \sum_{k=1}^N \frac{1}{z_k} \int_{e_k} (u_1 - U_{k,1}) (\bar{v} - \bar{V}_k) \right) ds \\ &\quad + c_2 \left( \int_{\Omega} \sigma \nabla u_2 \cdot \nabla \bar{v} dx + \sum_{k=1}^N \frac{1}{z_k} \int_{e_k} (u_2 - U_{k,2}) (\bar{v} - \bar{V}_k) \right) ds \\ &= c_1 B((u_1, U_1), (v, V)) + c_2 B((u_2, U_2), (v, V)) \end{aligned}$$

and

$$\begin{aligned}
B((v, V), c_1(u_1, U_1) + c_2(u_2, U_2)) &= \int_{\Omega} \sigma \nabla v \cdot \nabla (\overline{c_1 u_1 + c_2 u_2}) dx \\
&\quad + \sum_{k=1}^N \frac{1}{z_k} \int_{e_k} (v - V_k) (\overline{c_1 u_1 + c_2 u_2} - \overline{(c_1 U_1 + c_2 U_2)_k}) ds \\
&= \int_{\Omega} \sigma \nabla v \cdot \nabla \overline{c_1 u_1} + \sigma \nabla v \cdot \nabla \overline{c_2 u_2} dx \\
&\quad + \sum_{k=1}^N \frac{1}{z_k} \int_{e_k} \overline{c_1} (v - V_k) (\overline{u_1} - \overline{U_{1k}}) + \overline{c_2} (v - V_k) (\overline{u_2} - \overline{U_{2k}}) ds \\
&= \overline{c_1} \left( \int_{\Omega} \sigma \nabla v \cdot \nabla \overline{u_1} dx + \sum_{k=1}^N \frac{1}{z_k} \int_{e_k} (v - V_k) (\overline{u_1} - \overline{U_{k,1}}) \right) ds \\
&\quad + \overline{c_2} \left( \int_{\Omega} \sigma \nabla v \cdot \nabla \overline{u_2} dx + \sum_{k=1}^N \frac{1}{z_k} \int_{e_k} (v - V_k) (\overline{u_2} - \overline{U_{k,2}}) \right) ds \\
&= \overline{c_1} B((v, V), (u_1, U_1)) + \overline{c_2} B((v, V), (u_2, U_2))
\end{aligned}$$

and thus we have shown that  $B$  is sesquilinear. **(ii)** Next we show boundedness of  $B$ :

$$\begin{aligned}
|B((u, U), (v, V))| &= \left| \int_{\Omega} \sigma \nabla u \cdot \nabla \overline{v} dx + \sum_{k=1}^N \frac{1}{z_k} \int_{e_k} (u - U_k) (\overline{v} - \overline{V_k}) ds \right| \\
&\leq \int_{\Omega} |\sigma| |\nabla u| \cdot |\nabla \overline{v}| dx + \sum_{k=1}^N \frac{1}{|z_k|} \int_{e_k} |u - U_k| |\overline{v} - \overline{V_k}| ds \\
&\leq \sigma_1 \int_{\Omega} |\nabla u| \cdot |\nabla \overline{v}| dx + \frac{1}{Z} \sum_{k=1}^N \int_{e_k} |u - U_k| |\overline{v} - \overline{V_k}| ds \\
&\leq C \cdot \left( \int_{\Omega} |\nabla u| \cdot |\nabla v| dx + \sum_{k=1}^N \int_{e_k} |u - U_k| |v - V_k| ds \right),
\end{aligned}$$

where  $C = \max\{\sigma_1, \frac{1}{Z}\}$ . Using Cauchy-Schwarz Inequality:

$$\begin{aligned}
\int_{\Omega} |\nabla u| \cdot |\nabla v| dx &\leq \left( \int_{\Omega} |\nabla u|^2 dx \right)^{1/2} \left( \int_{\Omega} |\nabla v|^2 dx \right)^{1/2} \\
&= \|\nabla u\|_{L^2(\Omega)} \cdot \|\nabla v\|_{L^2(\Omega)}.
\end{aligned} \tag{2.38}$$

For any  $k$ :

$$\int_{e_k} |u - U_k| |v - V_k| ds \leq \left( \int_{e_k} |u - U_k|^2 dx \right)^{1/2} \left( \int_{e_k} |v - V_k|^2 dx \right)^{1/2} \tag{2.39}$$

and by Hölder's Inequality for sums:

$$\begin{aligned} & \sum_{k=1}^N \left( \int_{e_k} |u - U_k|^2 ds \right)^{1/2} \left( \int_{e_k} |v - V_k|^2 ds \right)^{1/2} \\ & \leq \left( \sum_{k=1}^N \int_{e_k} |u - U_k|^2 ds \right)^{1/2} \left( \sum_{k=1}^N \int_{e_k} |v - V_k|^2 ds \right)^{1/2}. \end{aligned} \quad (2.40)$$

Thus we have:

$$\begin{aligned} |B((u, U), (v, V))|^2 & \leq C (\|\nabla u\|_{L^2(\Omega)} \cdot \|\nabla v\|_{L^2(\Omega)} \\ & \quad + \left( \sum_{k=1}^N \int_{e_k} |u - U_k|^2 ds \right)^{1/2} \left( \sum_{k=1}^N \int_{e_k} |v - V_k|^2 ds \right)^{1/2})^2 \\ & \leq C (\|\nabla u\|_{L^2(\Omega)}^2 \cdot \|\nabla v\|_{L^2(\Omega)}^2 \\ & \quad + \left( \sum_{k=1}^N \int_{e_k} |u - U_k|^2 ds \right) \left( \sum_{k=1}^N \int_{e_k} |v - V_k|^2 ds \right)) \\ & \quad + 2C (\|\nabla u\|_{L^2(\Omega)} \cdot \|\nabla v\|_{L^2(\Omega)} \\ & \quad \cdot \left( \sum_{k=1}^N \int_{e_k} |u - U_k|^2 ds \right)^{1/2} \left( \sum_{k=1}^N \int_{e_k} |v - V_k|^2 ds \right)^{1/2}) \\ & \leq C (\|\nabla u\|_{L^2(\Omega)}^2 \cdot \|\nabla v\|_{L^2(\Omega)}^2 \\ & \quad + \left( \sum_{k=1}^N \int_{e_k} |u - U_k|^2 ds \right) \left( \sum_{k=1}^N \int_{e_k} |v - V_k|^2 ds \right)) \\ & \quad + C \left( \|\nabla u\|_{L^2(\Omega)}^2 \left( \sum_{k=1}^N \int_{e_k} |v - V_k|^2 ds \right) \right. \\ & \quad \left. + \|\nabla v\|_{L^2(\Omega)}^2 \left( \sum_{k=1}^N \int_{e_k} |u - U_k|^2 ds \right) \right) \\ & = C \left( \|\nabla u\|_{L^2(\Omega)}^2 + \sum_{k=1}^N \int_{e_k} |u - U_k|^2 ds \right) \\ & \quad \cdot \left( \|\nabla v\|_{L^2(\Omega)}^2 + \sum_{k=1}^N \int_{e_k} |v - V_k|^2 ds \right) \\ & = C \| (u, U) \|_*^2 \| (v, V) \|_*^2, \end{aligned}$$

i.e.  $B$  is bounded.

(iii) Finally we show that  $B$  is coercive. Since  $|\sigma| \leq \sigma_1$  and  $\operatorname{Re}(z_k) > Z$  we can choose  $d$  s.t.  $|\frac{\sigma}{d}| < 1$  and  $|\frac{1}{z_k \cdot d}| < 1$  for all  $k$ . Then

$$\begin{aligned} |B((u, U), (u, U))| &= \left| \int_{\Omega} \sigma \nabla u \cdot \nabla \bar{u} \, dx + \sum_{k=1}^N \frac{1}{z_k} \int_{e_k} (u - U_k)(\bar{u} - \bar{U}_k) \, ds \right| \\ &\geq d \cdot \left( \int_{\Omega} |\nabla u|^2 \, dx + \sum_{k=1}^N \int_{e_k} |u - U_k|^2 \, ds \right) \\ &= d \|(u, U)\|_*^2, \end{aligned}$$

and thus  $B$  is coercive.  $\square$

We have now shown that  $B$  satisfies the hypotheses of the Lax-Milgram Theorem on  $(\mathcal{V}, \|\cdot\|_*)$ . By Lemma 2.3 it thus also does on  $(\mathcal{V}, \|\cdot\|_{\mathcal{V}})$ . Therefore we can now establish the unique solvability for the variational problem (2.1).

**THEOREM 2.5** *Under the assumptions of  $\Omega$ ,  $\sigma$  and  $z_k$  given in the beginning of the chapter, there exists, for any  $\{I_k\}_{k=1}^N$  satisfying  $\sum_{k=1}^N I_k = 0$ , a unique  $(u, U) \in \mathcal{V}$  s.t.;*

$$B((u, U), (v, V)) = \sum_{k=1}^N I_k \bar{V}_k, \quad \forall (v, V) \in \mathcal{V}, \quad (2.41)$$

where  $B$  is defined as in (2.2).

PROOF. By the assumptions, the previous proposition implies that  $B$  satisfies the Lax-Milgram criteria on  $(\mathcal{V}, \|\cdot\|_*)$ . To apply Lax-Milgram, we are therefore left to show that the functional:

$$f : \mathcal{V} \rightarrow \mathbb{C}, \quad f(v, V) = \sum_{k=1}^N I_k \bar{V}_k \quad (2.42)$$

is well-defined, anti-linear and continuous. It is clearly anti-linear, since for  $(v, V)$  and  $(w, W)$  in  $\mathcal{V}$  and  $(c_1, c_2) \in \mathbb{C}^2$ :

$$f(c_1(v, V) + c_2(w, W)) = \sum_{k=1}^N I_k \cdot \overline{(c_1 V_k + c_2 W_k)} \quad (2.43)$$

$$= \bar{c}_1 \sum_{k=1}^N I_k \bar{V}_k + \bar{c}_2 \sum_{k=1}^N I_k \bar{W}_k \quad (2.44)$$

$$= \bar{c}_1 f(v, V) + \bar{c}_2 f(w, W). \quad (2.45)$$

To show well-definedness, note that for any  $c \in \mathbb{C}$ ;

$$f(v + c, V + c) = \sum_{k=1}^N I_k \overline{V_k} + \bar{c} \sum_{k=1}^N I_k = \sum_{k=1}^N I_k \overline{V_k} = f(v, V). \quad (2.46)$$

To show boundedness let  $\epsilon > 0$  be arbitrary, and choose  $c$  s.t.:

$$(\|v - c\|_{H^1(\Omega)}^2 + \|V - c_N\|_{\mathbb{C}}^2)^{1/2} \leq \|(v, V)\|_{\mathcal{V}} + \epsilon. \quad (2.47)$$

Then

$$|f(v, V)| = |f(v - c, V - c)| = \left| \sum_{k=1}^N I_k (\overline{V_k - c}) \right| \quad (2.48)$$

$$\leq \|I\|_{\mathbb{C}^N} \cdot \|V - c\|_{\mathbb{C}^N} \leq \|I\|_{\mathbb{C}^N} (\|(v, V)\|_{\mathcal{V}} + \epsilon). \quad (2.49)$$

Since it holds for any arbitrary  $\epsilon > 0$ , we conclude  $f$  is bounded, thus continuous. Hence, by Theorem 2.2, there exists a unique  $(u, U) \in \mathcal{V}$  satisfying (2.41).  $\square$

We have now shown uniqueness of the problem in  $\mathcal{V}$ , which is uniqueness up to a constant. To establish uniqueness in  $\mathcal{H}$  we need a new criteria. This is carried out in the next corollary.

**COROLLARY 2.6** *If the assumptions from Theorem 2.5 holds and furthermore we specify that  $\sum_{k=1}^N U_k = 0$ , then the forward problem, has a unique solution in  $\mathcal{H}$ .*

PROOF. From the previous Theorem 2.5, we know there exists a unique solution  $(u, U)$  in  $\mathcal{V}$ . Thus there are infinitely many solutions in  $\mathcal{H}$ , which only differs by a constant. Say one of these solutions is  $(u, U)$ . Then  $U$  must satisfy  $\sum_{k=1}^N U_k = 0$ . For any  $c$ , another solution is  $(u + c, U + c_N)$ . But since  $\sum_{k=1}^N U_k + c = c \cdot N \neq 0$  this solution does not satisfy  $\sum_{k=1}^N U_k = 0$ . Hence there is a unique solution of the forward problem in  $\mathcal{H}$  provided that  $\sum_{k=1}^N U_k = 0$ .  $\square$

We have now established existence and uniqueness of the forward problem via Lax-Milgram. In the next section we will establish unique solvability by another approach.

## 2.3 Unique solvability of the forward problem via minimization

In this section we will present a second proof that the forward problem is uniquely solvable. This proof requires some further restrictions to the parameters  $\sigma$ ,  $z_k$  and the space  $\mathcal{H}$ . The new definition of  $\mathcal{H}$ , which we will use from now on and throughout the thesis is:

$$\mathcal{H} := \{(u, U) \in H^1(\Omega) \times \mathbb{R}^N \mid U_1 + \dots + U_N = 0\}. \quad (2.50)$$

Regarding  $\sigma$  and  $z_k$  we assume that these are real valued functions defined on  $\Omega$  and that there exists an  $\epsilon > 0$  s.t.

$$\epsilon < \sigma < \frac{1}{\epsilon} \quad \text{and} \quad \epsilon < z_k < \frac{1}{\epsilon} \quad \text{for all } k = 1, \dots, N. \quad (2.51)$$

These assumptions on  $\sigma$  and  $z_k$  will be the one used throughout the thesis.

The main result of this section establishes a 1-to-1 correspondence between solutions of the forward problem and minimizers of the functional  $F_\sigma : \mathcal{H} \rightarrow \mathbb{R}$  defined by:

$$F_\sigma(u, U) = \frac{1}{2} \int_{\Omega} \sigma |\nabla u|^2 dx + \frac{1}{2} \sum_{k=1}^N \int_{e_k} \frac{1}{z_k} (u - U_k)^2 ds - \sum_{k=1}^N I_k U_k. \quad (2.52)$$

Notice that

$$F_\sigma(u, U) = B((u, U), (u, U)) - \sum_{k=1}^N I_k U_k, \quad (2.53)$$

where  $B$  was defined in (2.2).

In this section we equip the space  $\mathcal{H}$  with the inner product:

$$\langle (u, U), (v, V) \rangle_{\mathcal{H}} := \int_{\Omega} uv \, dx + \int_{\Omega} \nabla u \cdot \nabla v \, dx + \sum_{k=1}^N U_k V_k \quad (2.54)$$

and the associated induced norm is:

$$\|(u, U)\|_{\mathcal{H}} = \left( \int_{\Omega} u^2 dx + \int_{\Omega} |\nabla u|^2 dx + \sum_{k=1}^N U_k^2 \right)^{1/2}. \quad (2.55)$$

As a start, we will prove a Proposition, which will be useful later on.

**PROPOSITION 2.7** *There exists a  $C > 0$ , depending on  $\Omega$  and the electrodes  $\{e_k\}_{k=1}^N$ , s.t. for any  $(u, U) \in \mathcal{H}$ , the below inequality holds:*

$$\int_{\Omega} u^2 dx + \sum_{k=1}^N U_k^2 \leq C \left( \int_{\Omega} |\nabla u|^2 dx + \sum_{k=1}^N \int_{e_k} (u - U_k)^2 ds \right). \quad (2.56)$$

PROOF. We prove this by showing that:

$$\kappa := \inf_{(u, U) \in \mathcal{H}} \frac{\int_{\Omega} |\nabla u|^2 dx + \sum_{k=1}^N \int_{e_k} (u - U_k)^2 ds}{\int_{\Omega} |\nabla u|^2 dx + \int_{\Omega} u^2 dx + \sum_{k=1}^N U_k^2} > 0. \quad (2.57)$$

This is shown by contradiction. So assume  $\kappa = 0$ . Then there must exist a sequence  $\{(u^n, U^n)\}_{n=1}^{\infty}$  s.t.

$$\lim_{n \rightarrow \infty} \int_{\Omega} |\nabla u^n|^2 dx + \sum_{k=1}^N \int_{e_k} (u^n - U_k^n)^2 ds = 0. \quad (2.58)$$

The statement in (2.58) is equivalent to:

$$\lim_{n \rightarrow \infty} \int_{\Omega} |\nabla u^n|^2 dx = 0 \quad (2.59)$$

$$\lim_{n \rightarrow \infty} \int_{e_k} (u^n - U_k^n)^2 ds = 0 \quad \text{for any } k = 0, \dots, N. \quad (2.60)$$

Without loss of generality we can assume that the elements of the sequence has norm 1,  $\|(u^n, U^n)\|_{\mathcal{H}} = 1$ . The unit sphere is compact in  $\{U \in \mathbb{R}^N | U_1 + \dots + U_N = 0\}$ , and by Theorem A.6 the unit sphere is weakly compact in  $H^1(\Omega)$ . Therefore there exists  $(u, U) \in \mathcal{H}$  with  $\|(u, U)\|_{\mathcal{H}} = 1$  and a subsequence  $\{(u^{n_j}, U^{n_j})\}_{j=1}^{\infty}$  of  $\{(u^n, U^n)\}_{n=1}^{\infty}$  such that

$$u^{n_j} \rightharpoonup u \quad \text{in } H^1(\Omega) \quad \text{as } j \rightarrow \infty \quad (2.61)$$

$$U^{n_j} \rightarrow U \quad \text{as } j \rightarrow \infty. \quad (2.62)$$

Since  $\{u^{n_j}\}$  is bounded in  $H^1(\Omega)$  the trace theorem (Theorem A.5) implies that  $\{u^{n_j}|_{e_k}\}$  is bounded in  $H^{1/2}(e_k)$ , hence in  $L^2(e_k)$  and  $L^1(e_k)$ , for each  $k = 1, \dots, N$ . For any  $k$  we have that:

$$\begin{aligned} \int_{e_k} (u^{n_j} - U_k)^2 ds &= \int_{e_k} [(u^{n_j} - U_k^{n_j})^2 + 2u^{n_j}(U_k^{n_j} - U_k) + U_k^2 - (U_k^{n_j})^2] ds \\ &= \int_{e_k} (u^{n_j} - U_k^{n_j})^2 ds \\ &\quad + 2(U_k^{n_j} - U_k) \int_{e_k} u^{n_j} ds + |e_k|(U_k^2 - (U_k^{n_j})^2) \end{aligned}$$

Using (2.60) on the first part above and (2.62) on the last two parts, we conclude that

$$\lim_{j \rightarrow \infty} \int_{e_k} (u^{n_j} - U_k)^2 ds = 0. \quad (2.63)$$

Notice that this only holds since  $u$  is bounded in  $L^1(e_k)$ . Thus  $u^{n_j}|_{e_k} \rightarrow U_k$  in  $L^2(e_k)$  and by the trace theorem  $u^{n_j}|_{e_k} \rightarrow u|_{e_k}$  in  $H^{1/2}(e_k)$ , thus also in  $L^2(e_k)$ . Therefore by uniqueness of the limit we have  $u|_{e_k} = U_k$  for any  $k = 0, \dots, N$ . Furthermore

$$\int_{\Omega} |\nabla(u^{n_j} - u)|^2 dx = \int_{\Omega} |\nabla u^{n_j}|^2 dx + \int_{\Omega} |\nabla u|^2 dx - 2 \int_{\Omega} \nabla u^{n_j} \cdot \nabla u dx \quad (2.64)$$

$$\rightarrow 0 + \int_{\Omega} |\nabla u|^2 dx - 2 \int_{\Omega} |\nabla u|^2 dx = - \int_{\Omega} |\nabla u|^2 dx, \quad (2.65)$$

as  $j \rightarrow \infty$ . Now, since  $\int_{\Omega} |\nabla(u^{n_j} - u)|^2 dx \geq 0$ , we must have  $\int_{\Omega} |\nabla u|^2 dx = 0$ , thus is  $u$  constant in  $\bar{\Omega}$ . Hence  $U_1 = \dots = U_N = u$ . But since  $U_1 + \dots + U_N = 0$ , we must have  $u = U_1 = \dots = U_N = 0$ , which contradicts with  $\|(u, U)\|_{\mathcal{H}} = 1$ . Therefore (2.57) holds true. Hence for any  $(u, U) \in \mathcal{H}$ ,

$$\frac{\int_{\Omega} |\nabla u|^2 dx + \sum_{k=1}^N \int_{e_k} (u - U_k)^2 ds}{\int_{\Omega} |\nabla u|^2 dx + \int_{\Omega} u^2 dx + \sum_{k=1}^N U_k^2} \geq \kappa. \quad (2.66)$$

By  $\int_{\Omega} |\nabla u|^2 dx \geq 0$ ,

$$\frac{\int_{\Omega} |\nabla u|^2 dx + \sum_{k=1}^N \int_{e_k} (u - U_k)^2 ds}{\int_{\Omega} u^2 dx + \sum_{k=1}^N U_k^2} \geq \kappa, \quad (2.67)$$

which gives us

$$\frac{1}{\kappa} \left( \int_{\Omega} |\nabla u|^2 dx + \sum_{k=1}^N \int_{e_k} (u - U_k)^2 ds \right) \geq \int_{\Omega} u^2 dx + \sum_{k=1}^N U_k^2 \quad (2.68)$$

and we have shown (2.56).  $\square$

We will use this result when proving the next Proposition, which states some properties of  $F_{\sigma}$ . Here we will show that  $F_{\sigma}$  is strictly convex, Gateaux differentiable and coercive.

**PROPOSITION 2.8** *The functional  $F_{\sigma} : \mathcal{H} \rightarrow \mathbb{R}$  given in (2.52) has the following properties:*

(a)  $F_{\sigma}$  is strictly convex.



(b)  $F_\sigma$  is Gateaux-differentiable in  $\mathcal{H}$  and the derivative at  $(u, U)$  in the direction of  $(v, V)$  is:

$$\begin{aligned} D_G(F_\sigma((u, U)); (v, V)) &= \int_{\Omega} \sigma \nabla u \cdot \nabla v dx + \sum_{k=1}^N \int_{e_k} \frac{1}{z_k} (u - U_k)(v - V_k) ds - \sum_{k=1}^N I_k V_k. \end{aligned} \quad (2.69)$$

(c)  $F_\sigma$  is coercive in the sense that there exists a constant  $c > 0$ , depending on  $\kappa$  from (2.57) and  $\epsilon, s.t.$

$$F_\sigma(u, U) \geq \frac{c}{2} \|(u, U)\|_{\mathcal{H}}^2 - \frac{1}{2c} \sum_{k=1}^N I_k^2. \quad (2.70)$$

Notice that the first two parts on the right hand side of (2.69) sum up to  $B((u, U), (v, V))$ , defined in (2.2), and the last part is the right hand side of (2.1).

PROOF. (a) The first two terms of  $F_\sigma$ ,  $\int_{\Omega} \sigma |\nabla u|^2 dx$  and  $\int_{e_k} \frac{1}{z_k} (u - U_k)^2 ds$ , are quadratic, thus strictly convex. The last term,  $\sum_{k=1}^N I_k U_k$ , is linear, hence convex. Therefore  $F_\sigma$  is strictly convex.

(b) In this proof we will find the Gateaux derivative of  $F_\sigma$  at the point  $(u, U)$  in direction of  $(v, V)$ , given by:

$$D_G(F_\sigma((u, U)); (v, V)) = \lim_{\epsilon \rightarrow 0} \frac{F_\sigma((u, U) + \epsilon(v, V)) - F_\sigma(u, U)}{\epsilon}. \quad (2.71)$$

The first part  $F_\sigma((u, U) + \epsilon(v, V))$  can be seen as:

$$\begin{aligned}
& F_\sigma((u, U) + \epsilon(v, V)) \\
&= \frac{1}{2} \int_{\Omega} \sigma |\nabla(u + \epsilon v)|^2 dx + \frac{1}{2} \sum_{k=1}^N \int_{e_k} \frac{1}{z_k} (u + \epsilon v - U_k - \epsilon V_k)^2 ds \\
&\quad - \sum_{k=1}^N I_k (U_k + \epsilon V_k) \\
&= \frac{1}{2} \int_{\Omega} \sigma |\nabla u|^2 + \epsilon^2 \sigma |\nabla v|^2 + 2\sigma \nabla u \cdot \nabla v dx \\
&\quad + \frac{1}{2} \sum_{k=1}^N \int_{e_k} \frac{1}{z_k} [(u - U_k)^2 + \epsilon^2 (v - V_k)^2 + 2\epsilon(u - U_k)(v - V_k)] ds \\
&\quad - \sum_{k=0}^N I_k U_k + \epsilon I_k V_k \\
&= F_\sigma(u, U) + \epsilon^2 \left( F_\sigma(v, V) + \sum_{k=1}^N I_k V_k \right) \\
&\quad + \epsilon \left( \int_{\Omega} \sigma \nabla u \cdot \nabla v dx + \sum_{k=1}^N \int_{e_k} \frac{1}{z_k} (u - U_k)(v - V_k) ds - \sum_{k=1}^N I_k V_k \right) \\
&= F_\sigma(u, U) + \epsilon^2 \left( F_\sigma(v, V) + \sum_{k=1}^N I_k V_k \right) \\
&\quad + \epsilon \left( B((u, U), (v, V)) - \sum_{k=1}^N I_k V_k \right).
\end{aligned}$$

Hence the Gateaux derivative is:

$$\begin{aligned}
& D_G(F_\sigma((u, U)); (v, V)) \\
&= \lim_{\epsilon \rightarrow 0} \frac{\epsilon^2 \left( F_\sigma(v, V) + \sum_{k=1}^N I_k V_k \right) + \epsilon \left( B((u, U), (v, V)) - \sum_{k=1}^N I_k V_k \right)}{\epsilon} \\
&= \lim_{\epsilon \rightarrow 0} \left( \epsilon \left( F_\sigma(v, V) + \sum_{k=1}^N I_k V_k \right) + B((u, U), (v, V)) - \sum_{k=1}^N I_k V_k \right) \\
&= B((u, U), (v, V)) - \sum_{k=1}^N I_k V_k \\
&= \int_{\Omega} \sigma \nabla u \cdot \nabla v dx + \sum_{k=1}^N \int_{e_k} \frac{1}{z_k} (u - U_k)(v - V_k) ds - \sum_{k=1}^N I_k V_k.
\end{aligned}$$

(c) By (2.66) from the proof of Proposition 2.7 we have

$$\int_{\Omega} |\nabla u|^2 dx + \sum_{k=1}^N \int_{e_k} (u - U_k)^2 ds \geq \kappa \left( \int_{\Omega} |\nabla u|^2 dx + \int_{\Omega} u^2 dx + \sum_{k=1}^N U_k^2 \right) \quad (2.72)$$

$$= \kappa \|(u, U)\|_{\mathcal{H}}^2. \quad (2.73)$$

We have that  $\epsilon \leq \sigma$ ,  $z_k \leq \epsilon^{-1}$  for all  $k$ , i.e.  $\epsilon^{-1}\sigma \geq 1$  and  $\epsilon^{-1}z_k^{-1} \geq 1$ . Thus

$$\begin{aligned} \int_{\Omega} |\nabla u|^2 dx + \sum_{k=1}^N \int_{e_k} (u - U_k)^2 ds \\ \leq \int_{\Omega} \epsilon^{-1}\sigma |\nabla u|^2 dx + \sum_{k=1}^N \int_{e_k} \epsilon^{-1} \frac{1}{z_k} (u - U_k)^2 ds. \end{aligned} \quad (2.74)$$

So

$$\begin{aligned} \frac{\epsilon}{2} \left( \int_{\Omega} |\nabla u|^2 dx + \sum_{k=1}^N \int_{e_k} (u - U_k)^2 ds \right) \\ \leq \frac{1}{2} \int_{\Omega} \sigma |\nabla u|^2 dx + \frac{1}{2} \sum_{k=1}^N \int_{e_k} \frac{1}{z_k} (u - U_k)^2 ds \\ = F_{\sigma}(u, U) + \sum_{k=1}^N I_k U_k. \end{aligned}$$

Combining this with (2.73), we get

$$F_{\sigma}(u, U) \geq \kappa \frac{\epsilon}{2} \|(u, U)\|_{\mathcal{H}}^2 - \sum_{k=1}^N I_k U_k. \quad (2.75)$$

Let us from now denote  $c = \kappa \frac{\epsilon}{2}$ . By the definition of the norm  $\|\cdot\|_{\mathcal{H}}$  in (2.55),

$$\|(u, U)\|_{\mathcal{H}}^2 = \|u\|_{H^1(\Omega)}^2 + \sum_{k=1}^N U_k^2. \quad (2.76)$$

Using that  $(x - y)^2 \geq \frac{1}{2}x^2 - y^2$ , we get

$$c \sum_{k=1}^N U_k^2 - \sum_{k=1}^N I_k U_k = c \sum_{k=1}^N \left( U_k - \frac{1}{2c} I_k \right)^2 - \frac{1}{4c} \sum_{k=1}^N I_k^2 \quad (2.77)$$

$$\geq c \sum_{k=1}^N \left( \frac{1}{2} U_k^2 - \frac{1}{4c^2} I_k^2 \right) - \frac{1}{4c} \sum_{k=1}^N I_k^2 \quad (2.78)$$

$$= \frac{c}{2} \sum_{k=1}^N U_k^2 - \frac{1}{2c} \sum_{k=1}^N I_k^2. \quad (2.79)$$

Combining the above with (2.75) we have

$$F_\sigma(u, U) \geq \frac{c}{2} \|(u, U)\|_{\mathcal{H}}^2 - \frac{1}{2c} \sum_{k=1}^N I_k^2, \quad (2.80)$$

which finishes the proof.  $\square$

The properties of  $F_\sigma$  will now be useful when establishing uniqueness. First we will show how a solution of the forward problem relates to  $F_\sigma$ .

**PROPOSITION 2.9** *Let  $(u, U) \in \mathcal{H}$ . Then,  $(u, U)$  is a solution to the forward problem with conductivity  $\sigma$  if and only if*

$$D_G(F_\sigma((u, U)); (v, V)) = 0 \quad \forall (v, V) \in \mathcal{H}. \quad (2.81)$$

PROOF. Proposition 2.8 (2) states that

$$D_G(F_\sigma((u, U)); (v, V)) = B((u, U), (v, V)) - \sum_{k=1}^N I_k V_k \quad (2.82)$$

and by Proposition 2.1,  $(u, U)$  solves the forward problem if and only if

$$B((u, U), (v, V)) = \sum_{k=1}^N I_k V_k \quad \forall (v, V) \in \mathcal{H}. \quad (2.83)$$

This completes the proof.  $\square$

Now we are ready to state the main result of this section. Using  $F_\sigma$  we show how the forward problem has a unique solution, and that this solution can be found by minimizing  $F_\sigma$ .

**THEOREM 2.10**  *$F_\sigma$  has a unique minimizer  $(u, U)$  in  $\mathcal{H}$  and that minimizer is a solution of the forward problem. Conversely, if the forward problem has a solution, that solution is a minimizer of  $F_\sigma$  and is hence unique.*

PROOF. First let us show that  $F_\sigma$  has a unique minimizer in  $\mathcal{H}$ . Let

$$d := \inf_{(u, U) \in \mathcal{H}} F_\sigma(u, U) \quad (2.84)$$

and let  $\{(u^n, U^n)\}_{n=1}^\infty \subset \mathcal{H}$  be a minimizing sequence for  $F_\sigma$  s.t.

$$d \leq F_\sigma(u^n, U^n) \leq d + \frac{1}{n}. \quad (2.85)$$

Combining (2.75), (2.76) and (2.77), there exists a  $c > 0$  s.t.

$$F_\sigma(u, U) \geq c\|u\|_{H^1(\Omega)}^2 + c \sum_{k=1}^N \left( U_k - \frac{1}{2c} I_k \right)^2 - \frac{1}{4c} \sum_{k=1}^N I_k^2 \quad (2.86)$$

$$\geq -\frac{1}{4c} \sum_{k=1}^N I_k^2, \quad (2.87)$$

for all  $(u, U) \in \mathcal{H}$ . Therefore  $d \neq -\infty$ . By Proposition 2.8 (c)

$$\lim_{\|(u, U)\|_{\mathcal{H}} \rightarrow \infty} F_\sigma(u, U) = \infty. \quad (2.88)$$

In view of (2.85) and (2.88) it follows that  $\{(u^n, U^n)\}_{n=1}^\infty$  is bounded. This in turn implies  $\{(u^n, U^n)\}_{n=1}^\infty$  is weakly compact (by Theorem A.6), i.e. there exists a subsequence  $\{(u^{n_j}, U^{n_j})\}_{j=1}^\infty$  such that

$$u^{n_j} \rightharpoonup u \text{ in } H^1(\Omega) \text{ and } U^{n_j} \rightarrow U \text{ in } \{U \in \mathbb{R}^N \mid U_1 + \dots + U_N = 0\} \quad (2.89)$$

for some  $(u, U) \in \mathcal{H}$ . By Proposition 2.8 (a) and (b),  $F_\sigma$  is convex and Gateaux differentiable at  $(u, U)$  in any direction, hence also in the direction of  $(u^{n_j} - u, U^{n_j} - U)$  for any  $j$ . Therefore

$$F_\sigma(u^{n_j}, U^{n_j}) \geq F_\sigma(u, U) + D_G(F_\sigma((u, U)); (u^{n_j} - u, U^{n_j} - U)) \quad (2.90)$$

and by the convergence (2.89)

$$D_G(F_\sigma((u, U)); (u^{n_j} - u, U^{n_j} - U)) \rightarrow 0 \text{ as } j \rightarrow \infty. \quad (2.91)$$

Thus as  $j \rightarrow \infty$ ,  $F_\sigma(u, U) \leq F_\sigma(u^{n_j}, U^{n_j}) \rightarrow d$ . Combining with (2.84),  $F_\sigma(u, U) = d$ . Thus  $(u, U)$  is a global minimizer of  $F_\sigma$ . It is unique by  $F_\sigma$  being strictly convex. Furthermore at  $(u, U)$ ,  $D_G(F_\sigma((u, U)); (v, V)) = 0$  for all  $(v, V) \in \mathcal{H}$ . Thus, by Proposition 2.9,  $(u, U)$  is a solution to the forward problem.

On the other hand, if  $(u, U)$  is a solution to the forward problem, we have, by Proposition 2.9, that  $D_G(F_\sigma((u, U)); (v, V)) = 0$  for all  $(v, V) \in \mathcal{H}$  and by convexity  $(u, U)$  must be a minimizer of  $F_\sigma$ . By strict convexity it is unique.  $\square$

We have now shown existence and uniqueness of the forward problem by two different approaches. In Chapter 4 we will study the forward problem by doing numerical experiments. In the next chapter we will study the inverse problem of finding the conductivity.



## CHAPTER 3

# Current Density Impedance Imaging

---

In this chapter we will discuss the inverse problem of finding the conductivity  $\sigma$ . We will characterize the non-uniqueness of the problem and to which extend we can find a solution to the problem.

By the previous chapter, there is a unique solution  $(u, U) \in \mathcal{H}$ , which solves the forward problem w.r.t.  $\sigma$  and  $\{I_k\}_{k=1}^N$ , in weak sense. In this Chapter we fix the conductivity  $\sigma$  and let  $(u, U)$  be the solution of the forward problem with this conductivity. We denote the magnitude of the current density by  $a$ ,  $a := \sigma|\nabla u|$ . The main goal of this section is to discuss if knowledge of  $a$  determines  $\sigma$  uniquely. By knowledge of  $a$  we define the functional  $G_a$  by:

$$G_a(v, V) = \int_{\Omega} a|\nabla v| dx + \sum_{k=1}^N \int_{e_k} \frac{1}{2z_k} (v - V_k)^2 ds - \sum_{k=1}^N I_k V_k. \quad (3.1)$$

Notice how the construction of  $G_a$  arises from  $F_{\sigma}$ .  $G_a(u, U)$  only differs from  $F_{\sigma}$  by  $\frac{1}{2} \int_{\Omega} a|\nabla u| dx$ .

### 3.1 Defining a minimal gradient problem

In this section we will show, that  $(u, U)$  is a minimizer of  $G_a$  given in (3.1).

**PROPOSITION 3.1** *For any  $(v, V)$  in  $\mathcal{H}$  it holds that*

$$G_a(v, V) \geq G_a(u, U), \quad (3.2)$$

*i.e.  $(u, U)$  is a minimizer of  $G_a$ .*

PROOF. We let  $(v, V) \in \mathcal{H}$ . Then

$$G_a(v, V) = \int_{\Omega} \sigma |\nabla u| |\nabla v| dx + \sum_{k=1}^N \int_{e_k} \frac{1}{2z_k} (v - V_k)^2 ds - \sum_{k=1}^N I_k V_k \quad (3.3)$$

$$\geq \int_{\Omega} \sigma \nabla u \cdot \nabla v dx + \sum_{k=1}^N \int_{e_k} \left( \frac{1}{2z_k} (v - V_k)^2 - \sigma \frac{\partial u}{\partial n} V_k \right) ds, \quad (3.4)$$

where the last inequality comes by  $u$  solving the forward problem, so (1.4) holds. Notice that if  $v = u$  we have equality in (3.4). Also  $\nabla \cdot \sigma \nabla u = 0$  in  $\Omega$  implies

$$\begin{aligned} \int_{\Omega} \sigma \nabla u \cdot \nabla v dx &= \int_{\partial\Omega} v \sigma \frac{\partial u}{\partial n} ds - \int_{\Omega} \nabla \cdot \sigma \nabla u v dx \\ &= \int_{\partial\Omega} v \sigma \frac{\partial u}{\partial n} ds = \sum_{k=1}^N \int_{e_k} v \sigma \frac{\partial u}{\partial n} ds, \end{aligned}$$

with the last equality coming from  $\sigma \frac{\partial u}{\partial n} = 0$  on  $\partial\Omega \setminus \cup_{k=1}^N e_k$ . Thus we have

$$G_a(v, V) \geq \sum_{k=1}^N \int_{e_k} \left( v \sigma \frac{\partial u}{\partial n} + \frac{1}{2z_k} (v - V_k)^2 - \sigma \frac{\partial u}{\partial n} V_k \right) ds \quad (3.5)$$

$$= \sum_{k=1}^N \int_{e_k} \frac{1}{z_k} \left( z_k \sigma \frac{\partial u}{\partial n} v + \frac{1}{2} (v - V_k)^2 - z_k \sigma \frac{\partial u}{\partial n} V_k \right) ds \quad (3.6)$$

$$= \sum_{k=1}^N \int_{e_k} \frac{1}{z_k} \left( -(u - U_k)(v - V_k) + \frac{1}{2} (v - V_k)^2 \right) ds, \quad (3.7)$$

with the last inequality coming from  $z_k \sigma \frac{\partial u}{\partial n} = U_k - u$ . At this point we observe that if  $v = u$ , we would have equality in (3.4) and (3.5) which implies that:

$$G_a(u, U) = \sum_{k=1}^N \left( -\frac{1}{2z_k} \right) \int_{e_k} (u - U_k)^2 ds. \quad (3.8)$$



We have that

$$((u - U_k) + (v - V_k))^2 \geq 0 \quad \Leftrightarrow \quad (v - V_k)^2 \geq 2(u - U_k)(v - V_k) - (u - U_k)^2$$

and therefore:

$$\begin{aligned} G_a(v, V) &\geq \sum_{k=1}^N \int_{e_k} \frac{1}{z_k} \left( -(u - U_k)(v - V_k) + (u - U_k)(v - V_k) - \frac{1}{2}(u - U_k)^2 \right) \\ &= \sum_{k=1}^N \int_{e_k} -\frac{1}{2z_k} (u - U_k)^2 ds = G_a(u, U) \end{aligned}$$

This concludes the proof.  $\square$

Using this result, we can show non-uniqueness of the inverse problem and furthermore characterize the non-uniqueness.

## 3.2 Characterization of non-uniqueness

In this section we will study the non-uniqueness of determining the unknown conductivity  $\sigma$ . The content of the first result is that knowledge of  $a$  alone does not suffice to uniquely determine  $\sigma$ . Moreover, this result furnishes a characterization of this non-uniqueness.

**THEOREM 3.2** *Let  $(\tilde{u}, \tilde{U})$  be the solution of the forward problem with conductivity  $\tilde{\sigma}$ . Assume  $\partial\Omega \in C^{1,\alpha}$  for some  $\alpha \in (0, 1)$  and  $\sigma, \tilde{\sigma} \in C^\alpha(\Omega; \mathbb{R})$ . Then, if*

$$\sigma|\nabla u| = \tilde{\sigma}|\nabla \tilde{u}| > 0 \text{ a.e. in } \Omega, \quad (3.9)$$

there exists a function  $\phi \in C^1(u(\Omega))$ , with  $\phi'(t) > 0$  a.e. s.t.

$$\tilde{u} = \phi \circ u \text{ in } \Omega \quad \text{and} \quad \tilde{\sigma} = \frac{\sigma}{\phi' \circ u} \text{ a.e. in } \Omega. \quad (3.10)$$

Furthermore for all  $k = 1, \dots, N$ :

$$\phi(t) = t - (U_k - \tilde{U}_k) \quad \text{for } t \in u(e_k) \quad (3.11)$$

PROOF. Because of (3.9), both  $(u, U)$  and  $(\tilde{u}, \tilde{U})$  minimize  $G_a$ , i.e.

$$G_a(u, U) = G_a(\tilde{u}, \tilde{U}). \quad (3.12)$$

Therefore by (3.7):

$$G_a(\tilde{u}, \tilde{U}) = \sum_{k=1}^N \int_{e_k} \frac{1}{z_k} \left( -(u - U_k)(\tilde{u} - \tilde{U}_k) + \frac{1}{2}(\tilde{u} - \tilde{U}_k)^2 \right) ds, \quad (3.13)$$

and

$$G_a(u, U) = -\frac{1}{2} \int_{e_k} \frac{1}{z_k} (u - U_k)^2 ds. \quad (3.14)$$

Thus

$$\begin{aligned} G_a(\tilde{u}, \tilde{U}) - G_a(u, U) &= \frac{1}{2} \sum_{k=1}^N \int_{e_k} \frac{1}{z_k} \left( (u - U_k)^2 + (\tilde{u} - \tilde{U}_k)^2 - 2(u - U_k)(\tilde{u} - \tilde{U}_k) \right) ds \\ &= \frac{1}{2} \sum_{k=1}^N \int_{e_k} \frac{1}{z_k} \left( (u - U_k) - (\tilde{u} - \tilde{U}_k) \right)^2 ds = 0 \end{aligned}$$

By  $z_k$ 's being strictly positive and  $\left( (u - U_k) - (\tilde{u} - \tilde{U}_k) \right)^2 \geq 0$  we have

$$\int_{e_k} \frac{1}{z_k} \left( (u - U_k) - (\tilde{u} - \tilde{U}_k) \right)^2 ds = 0 \quad \text{for all } k = 1, \dots, N.$$

Hence

$$(u - U_k) - (\tilde{u} - \tilde{U}_k) = 0 \quad \text{a.e. on } e_k, \quad (3.15)$$

i.e.

$$u - U_k = \tilde{u} - \tilde{U}_k \quad \text{a.e on } e_k \text{ for all } k = 1, \dots, N. \quad (3.16)$$

Since we also have equality in (3.4) when  $v = \tilde{u}$ :

$$\int_{\Omega} \sigma |\nabla u| |\nabla \tilde{u}| dx = \int_{\Omega} \sigma \nabla u \cdot \nabla \tilde{u} dx. \quad (3.17)$$

Thus

$$\int_{\Omega} \sigma (|\nabla u| |\nabla \tilde{u}| - \nabla u \cdot \nabla \tilde{u}) dx = 0. \quad (3.18)$$

Since  $\sigma$  is strictly positive in  $\Omega$  and  $|\nabla u| |\nabla \tilde{u}| - \nabla u \cdot \nabla \tilde{u} \geq 0$  we must therefore have

$$|\nabla u| |\nabla \tilde{u}| = \nabla u \cdot \nabla \tilde{u} \quad \text{a.e. in } \Omega. \quad (3.19)$$

We let  $S = \{x \in \Omega \mid |\nabla u(x)| = 0\} \cup \{x \in \Omega \mid |\nabla \tilde{u}(x)| = 0\}$ . Both  $u$  and  $\tilde{u}$  are differentiable, even  $C^{1,\alpha}$  in  $\Omega$ , by elliptic regularity (Theorem (A.4)), thus  $\nabla u$  and  $\nabla \tilde{u}$  are continuous in  $\Omega$ . Therefore  $S$  is closed in  $\Omega$  and by (3.9), it follows that  $\Omega \setminus S$  is dense in  $\Omega$ . By (3.9) and continuity, whenever  $\nabla u \neq 0$  or  $\nabla \tilde{u} \neq 0$ , we can write:

$$\nabla \tilde{u} = \mu \nabla u. \quad (3.20)$$

Here  $\mu$  is continuous on  $\Omega \setminus S$  and  $\mu > 0$ . Since  $\Omega \setminus S$  is dense in  $\Omega$ ,  $\mu$  can be extended continuously to all of  $\Omega$ .

We let  $L_t$  be a connected component of the level set of  $u$  with the value  $t \in u(\Omega \setminus S)$ . Differentiating in a tangential direction,  $v_t$ , to  $L_t$ , gives  $\nabla u \cdot v_t = 0$ . Thus by (3.20);  $\nabla \tilde{u} \cdot v_t = 0$ , i.e.  $\tilde{u}$  is constant on  $L_t$ . Notice that  $\tilde{u}$  is not necessarily the same constant on all the connected components of the level set of  $u$  with value  $t$ .

Explicitly, we can write, that for any  $x_0 \in \Omega \setminus S$ :

$$\tilde{u}|_{L(u^{-1}(u(x_0));x_0)} \equiv \text{constant}, \quad (3.21)$$

where  $L(u^{-1}(u(x_0));x_0)$  defines the connected component of the level set of  $u$ , with value  $u(x_0)$ , including  $x_0$ . Furthermore we can write  $\Omega \setminus S$  as:

$$\Omega \setminus S = \bigcup_{t \in u(\Omega \setminus S)} u^{-1}(t) = \bigcup_{t \in u(\Omega \setminus S)} \bigcup_{L_t \text{ of } u^{-1}(t)} L_t. \quad (3.22)$$

Thus:

$$u(\Omega \setminus S) = \bigcup_{t \in u(\Omega \setminus S)} \bigcup_{L_t \text{ of } u^{-1}(t)} u(L_t). \quad (3.23)$$

Defining  $\phi : u(\Omega \setminus S) \rightarrow \mathbb{R}$  by:

$$\phi|_{L(u^{-1}(u(x_0));x_0)} := \tilde{u}(x), \quad (3.24)$$

where  $x$  is any point in  $L(u^{-1}(u(x_0));x_0)$ . This is well-defined by (3.21) and hence:

$$\forall x \in \Omega \setminus S : \quad \phi(u(x)) = \tilde{u}(x). \quad (3.25)$$

Furthermore by  $\tilde{u}$  being continuous on  $\Omega$ , the preceding equality extends to hold on all of  $\Omega$ . Explicitly, we have:

$$\phi(u(x)) = \tilde{u}(x), \quad \text{for all } x \in \Omega. \quad (3.26)$$

Hence we have shown the first part of (3.10). Furthermore,  $\tilde{u}$  is differentiable, thus  $\phi$  is and

$$\nabla \tilde{u}(x) = \phi'(u(x)) \nabla u(x) \quad (3.27)$$

Since this holds for all  $x \in \Omega$ , (3.20) implies that  $\mu = \phi' \circ u$ , thus  $\phi'$  is continuous on  $u(\Omega)$ . Moreover  $\mu > 0$  on  $\Omega \setminus S$ , hence  $\phi' > 0$  on  $u(\Omega \setminus S)$ .

Using (3.9)

$$\sigma(x) |\nabla u(x)| = \tilde{\sigma}(x) |\nabla \tilde{u}(x)| = \tilde{\sigma}(x) \cdot (\phi' \circ u)(x) |\nabla u(x)|, \quad \forall x \in \Omega \setminus S. \quad (3.28)$$

Since  $|\nabla u| > 0$  on  $\Omega \setminus S$ :

$$\tilde{\sigma} = \frac{\sigma}{\phi' \circ u} \quad \text{on } \Omega \setminus S, \quad (3.29)$$

we have shown the second part of (3.10). Finally, by (3.16), for any  $k = 1, \dots, N$ :

$$\tilde{u}(x) = \phi(u(x)) = u(x) - (U_k - \tilde{U}_k) \quad \text{on } e_k, \quad (3.30)$$

or

$$\phi(t) = t - (U_k - \tilde{U}_k) \quad \text{for } t \in u(e_k) \quad (3.31)$$

and we have shown that (3.11) holds.  $\square$

Another result rises from the Theorem above. That is if the magnitude of the current densities of two pairs are identical, then so are the current density. This result is stated in the Corollary below.

**COROLLARY 3.3** *Let  $\tilde{\sigma}$  and  $(\tilde{u}, \tilde{U})$  be defined as in the previous Theorem. Let  $J := \sigma \nabla u$  and  $\tilde{J} := \tilde{\sigma} \nabla \tilde{u}$ . If*

$$|J| = |\tilde{J}| > 0 \quad \text{a.e. in } \Omega, \quad (3.32)$$

then

$$J = \tilde{J} \quad \text{in } \Omega. \quad (3.33)$$

**PROOF.** The proof of this is immediate from the previous Theorem. Using (3.10) and (3.27) we have:

$$\tilde{J} = \tilde{\sigma} \nabla \tilde{u} = \frac{\sigma}{\phi' \circ u} \nabla \tilde{u} = \sigma \nabla u = J \quad \text{in } \Omega \setminus S$$

Both  $J$  and  $\tilde{J}$  are continuous by elliptic regularity in  $\Omega$ , since  $\sigma, \tilde{\sigma} \in C^\alpha(\Omega)$  and  $u, \tilde{u} \in C^{1,\alpha}(\Omega)$ . Furthermore  $\Omega \setminus S$  is dense in  $\Omega$ , thus the above extends to hold in all of  $\Omega$ .  $\square$

Another result, which will be useful when reconstructing the conductivity is the Maximum Principle of the forward problem.

**PROPOSITION 3.4** (*Maximum principle*). *If  $(u, U)$  is a solution to the forward problem then  $u$  attains maximum,  $M$ , and minimum,  $m$ , on  $\bigcup_{k=1}^N e_k$ . Furthermore if  $\Gamma$  is a curve on the boundary of  $\Omega$  connecting all electrodes  $e_k$ , then  $u(\Gamma \cup \bigcup_{k=1}^N e_k) = u(\bar{\Omega})$ .*

PROOF. By the weak maximum principle, Theorem A.1,  $u$  attains its minimum and maximum on  $\bar{\Omega}$  on  $\partial\Omega$ . Thus there is a  $x_0 \in \partial\Omega$  s.t.  $u(x_0) = M$ . By Hopf's Lemma, Lemma A.2,  $\frac{\partial u}{\partial n}(x_0) > 0$ , and since  $u$  satisfies the boundary condition (1.3), we have  $x_0 \in \bigcup_{k=1}^N e_k$ . In the exact same way, the weak maximum principle states, that there exists a  $y_0 \in \partial\Omega$ , s.t.  $u(y_0) = m$ , and by Hopf's Lemma  $\frac{\partial u}{\partial n}(y_0) < 0$ , thus  $y_0 \in \bigcup_{k=1}^N e_k$ .

By the definition of  $\Gamma$ ,  $\Gamma \cup \bigcup_{k=1}^N e_k$  is connected. Therefore  $u(\Gamma \cup \bigcup_{k=1}^N e_k)$  is an interval, and by the previous result, it includes  $m$  and  $M$ . Thus  $u(\Gamma \cup \bigcup_{k=1}^N e_k) = [m, M] = u(\bar{\Omega})$ .  $\square$

With this Proposition, we are now ready to state and prove that if  $u$  and  $\tilde{u}$  relates in a certain way on  $\Gamma$ , and  $\sigma|\nabla u| = \tilde{\sigma}|\nabla \tilde{u}|$ , we have uniqueness of the inverse problem.

**THEOREM 3.5** *Let  $(\tilde{u}, \tilde{U})$  be the solution to the forward problem with conductivity  $\tilde{\sigma}$ . Let  $\sigma, \tilde{\sigma} \in C^\alpha(\bar{\Omega})$ , for some  $\alpha \in (0, 1)$ . We let  $\Gamma \subset \partial\Omega$  be a curve, connecting the electrodes. If*

$$\sigma|\nabla u| = \tilde{\sigma}|\nabla \tilde{u}| > 0 \quad \text{a.e. in } \Omega, \quad (3.34)$$

and there exists a constant  $C$  s.t.

$$u|_\Gamma - C = \tilde{u}|_\Gamma. \quad (3.35)$$

Then

$$u - C = \tilde{u} \quad \text{in } \bar{\Omega} \quad (3.36)$$

and

$$\sigma = \tilde{\sigma} \quad \text{in } \Omega. \quad (3.37)$$

PROOF. From Theorem 3.2:

$$\tilde{u} = \phi \circ u \quad \text{in } \Omega. \quad (3.38)$$

But now we assume that  $\sigma, \tilde{\sigma} \in C^\alpha(\bar{\Omega})$  instead of  $\sigma, \tilde{\sigma} \in C^\alpha(\Omega)$ , thus, by elliptic regularity, the above extends to hold in  $\bar{\Omega}$ , i.e.

$$\tilde{u} = \phi \circ u \quad \text{in } \bar{\Omega}. \quad (3.39)$$

And for any  $k = 1, \dots, N$ , let  $t \in u(e_k)$  be arbitrary. Then:

$$\phi(t) = t - (U_k - \tilde{U}_k) \quad (3.40)$$

Taking any  $x \in \Gamma$  we have:

$$u(x) - C = \tilde{u}(x) = \phi(u(x)). \quad (3.41)$$

Thus for any  $t \in u(\Gamma)$ :

$$\phi(t) = t - C. \quad (3.42)$$

Combining (3.40) with (3.42) and using that  $u$  is continuous on  $\bar{\Omega}$  gives us: For any  $x_0 \in \Gamma \cap e_k$ ,

$$C = U_k - \tilde{U}_k \quad \text{for all } k = 1, \dots, N \quad (3.43)$$

So on  $u(\Gamma \cup \bigcup_{k=1}^N e_k)$ ,  $\phi(t) = t - C$ . By the previous maximum principle  $u(\bar{\Omega}) = u(\Gamma \cup \bigcup_{k=1}^N e_k)$ , thus

$$\phi(t) = t - C \quad \text{in } u(\bar{\Omega}). \quad (3.44)$$

Hence for any  $x \in \bar{\Omega}$ :

$$\tilde{u}(x) = \phi(u(x)) = u(x) - C. \quad (3.45)$$

Therefore  $\nabla u = \nabla \tilde{u}$  in  $\Omega$ . Combining this with (3.34) and using the previous Corollary:

$$\sigma \nabla u = \tilde{\sigma} \nabla \tilde{u} \quad \text{in } \Omega, \quad (3.46)$$

thus  $\sigma = \tilde{\sigma}$  in  $\Omega$ . □

In practice it will probably not be straight forward to find a function  $\tilde{u}$ , which is a solution to the forward problem, s.t.  $\tilde{u} = u + C$  on  $\Gamma$ . Especially it seems difficult if one does not know  $u$  on  $\Gamma$ . Thus in order to solve the inverse problem it is not sufficient with knowledge of  $a$ . But we do know, that if we find a pair  $(\tilde{\sigma}, \tilde{u})$ , where  $(\tilde{u}, \tilde{U})$  is the solution of the forward problem with conductivity  $\tilde{\sigma}$ , there exists a function  $\phi$  connecting this pair to the true conductivity  $\sigma$  and voltage  $u$ . So if one can construct this  $\phi$ -function we can reconstruct the true conductivity. By the Maximum Principle, Proposition 3.4, knowledge of  $u$  and  $\tilde{u}$  on  $\Gamma \cup \bigcup_{k=1}^N e_k$ , where  $\Gamma$  is a curve connecting the electrodes gives us the range of  $u$  and  $\tilde{u}$  in the entire domain  $\bar{\Omega}$ . And thus we would be able to construct  $\phi$  by (3.10), and hence also  $\sigma$ . This will be considered in Chapter 5, when solving the inverse problem numerically.

# Experiments of the forward problem

---

In this chapter we will do some numerical experiments of the forward problem to support the theory from Chapter 2. Throughout this chapter we will use the unit square as domain,  $\Omega = \{(x, y) | 0 \leq x \leq 1, 0 \leq y \leq 1\}$ . This domain does not actually satisfy the conditions of the theory, which was based on domains with smooth boundary.

We will solve the forward problem numerically, by defining a regular mesh on  $\Omega$ . Such a mesh can be seen in Figure 4.1. The mesh is defined by parameters  $n_x$  and  $n_y$ , s.t.  $\Omega$  is divided into  $n_x$ -parts in  $x$ -direction and  $n_y$  parts in the direction of  $y$ . This gives  $n_x \cdot n_y$  square elements, which are then divided into two triangles. In all our experiments we will use  $n_x = n_y$ .

We seek a solution,  $(u, U)$ , to the forward problem, for which  $u$  is defined as a piecewise Lagrange polynomial of order 1. So for element  $i$ ,  $E_i$ , we seek a function  $v_i$ , s.t. on  $E_i$ ,  $v_i$  is a polynomial of order 1 and elsewhere  $v_i = 0$ . Our solution  $u$  to the forward problem will then satisfy  $u|_{E_i} = v_i$ .

Furthermore we want  $U$  to satisfy  $\sum_{k=1}^N U_k = 0$ . Due to this restriction we cannot use the variational formulation, (2.1), directly. In the next section, we will show two methods of treating this restriction. This is done for  $U \in \mathbb{R}^N$ ,

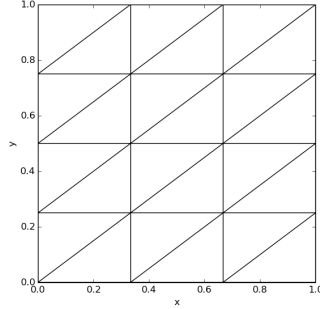


**Figure 4.1:** Example of a mesh on  $\Omega$ . Here with  $n_x = 3$  and  $n_y = 4$ .

since we in the experiments will work in a real space.

## 4.1 Implementing the CEM

As proved in 2.6, the forward problem has a unique solution provided  $\sum_{k=1}^N U_k = 0$ . There are two ways of implementing this criteria to the numerical solver.

The first one is as follows: Assume  $U \in \mathbb{R}^N$  and define  $U_N = -\sum_{k=1}^{N-1} U_k$ . Then  $\sum_{k=1}^N U_k = 0$  and our bilinear form  $B$  has the form:

$$\begin{aligned}
 B((u, U), (v, V)) &= \int_{\Omega} \sigma \nabla u \cdot \nabla v \, dx + \sum_{k=1}^{N-1} \frac{1}{z_k} \int_{e_k} (u - U_k)(v - V_k) \, ds \\
 &+ \frac{1}{z_N} \int_{e_N} \left( u + \sum_{k=1}^{N-1} U_k \right) \left( v + \sum_{k=1}^{N-1} V_k \right) \, ds.
 \end{aligned} \tag{4.1}$$

Similar the right hand side of (2.1) becomes

$$\sum_{k=1}^{N-1} I_k V_k - I_N \sum_{k=1}^{N-1} V_k. \tag{4.2}$$

Another way to do it is to expand the function space, in which we seek a solution, by adding an element  $c \in \mathbb{R}$ . Then  $(u, U)$  will solve the forward problem and satisfy  $\sum_{k=1}^N U_k = 0$  if

$$B((u, U, c), (v, V, d)) = \sum_{k=1}^N I_k V_k \quad \forall (v, V, d) \in H^1(\Omega) \times \mathbb{R}^N \times \mathbb{R}, \tag{4.3}$$



where

$$B((u, U, c), (v, V, d)) = \int_{\Omega} \sigma \nabla u \cdot \nabla v \, dx + \sum_{k=1}^N \frac{1}{z_k} \int_{e_k} (u - U_k)(v - V_k) \, ds + d \sum_{k=1}^N U_k + c \sum_{k=1}^N V_k. \quad (4.4)$$

Notice that when  $\nabla v = 0$  and  $V_k = 0$  for all  $k$ 's,  $\sum_{k=1}^N U_k = 0$ . Furthermore if  $d = 0$  and  $\sum_{k=0}^N V_k = 0$ ,  $(u, U)$  solves the forward problem.

We will in general consider two types of electrodes through the numerical experiments. The first type of electrodes are of length one and defined by:

$$e_1 = \{(x, y) | x = 0 \wedge 0 \leq y \leq 1\} \quad (4.5)$$

$$e_2 = \{(x, y) | x = 1 \wedge 0 \leq y \leq 1\} \quad (4.6)$$

$$e_3 = \{(x, y) | y = 0 \wedge 0 \leq x \leq 1\} \quad (4.7)$$

$$e_4 = \{(x, y) | y = 1 \wedge 0 \leq x \leq 1\} \quad (4.8)$$

These electrodes can only be used in the pairs  $(e_1, e_2)$  and  $(e_3, e_4)$  since we require that the electrodes have mutually disjoint closures. A basis of the currents on these electrodes are  $I_1 = I_3 = -I_2 = -I_4 = 1.0$ , which we will use through the experiments.

The second type of electrodes we will consider are:

$$e_1 = \{(x, y) | x = 0 \wedge 0.25 \leq y \leq 0.75\} \quad (4.9)$$

$$e_2 = \{(x, y) | x = 1 \wedge 0.25 \leq y \leq 0.75\} \quad (4.10)$$

$$e_3 = \{(x, y) | y = 0 \wedge 0.25 \leq x \leq 0.75\} \quad (4.11)$$

$$e_4 = \{(x, y) | y = 1 \wedge 0.25 \leq x \leq 0.75\} \quad (4.12)$$

These electrodes can be paired in any possible way, even with all four of them together. The basis, which we use, consist of three electrode pairs. These are given by their currents:  $(I_1, I_2) = (-1.0, 1.0)$ ,  $(I_3, I_4) = (-1.0, 1.0)$ ,  $(I_1, I_3) = (-1.0, 1.0)$ .

Regarding the impedances we let  $z_1 = z_2 = z_3 = z_4 = 1.0$  in all experiments.

Finally when solving the forward problem we would like to compare the solution with a true solution. We will from now on denote the true solution of the

forward problem by  $(u, U)$  and the numerically computed solution by  $(u_{n_x}, U_{n_x})$  depending on the mesh size  $n_x$ .

Throughout the experiments we will consider three types of errors, which is

$$\frac{\|u - u_{n_x}\|_{L^2}}{\|u\|_{L^2}}, \quad \frac{\|u - u_{n_x}\|_{H^1}}{\|u\|_{H^1}} \quad \text{and} \quad \frac{|U - U_{n_x}|}{|U|}. \quad (4.13)$$

These will, respectively, be referred to as the  $L^2$ -error,  $H^1$ -error and electrode-error.

## 4.2 Experiments with constant conductivity

In this section we will do some experiments when keeping the conductivity constant. We consider the electrodes given in (4.5) and (4.6).

As shown in Proposition A.7 in Appendix, the solution of the forward problem is in this scenario an affine function w.r.t.  $x$ . Thus there exists  $\alpha, \beta \in \mathbb{R}$  s.t.  $u(x, y) = \alpha x + \beta$ . We choose a constant conductivity of  $\sigma = 2.3$ . In Figure 4.2 is a plot of the true solution of the problem, as well as, the computed solution for a mesh with  $n_x = n_y = 128$ .

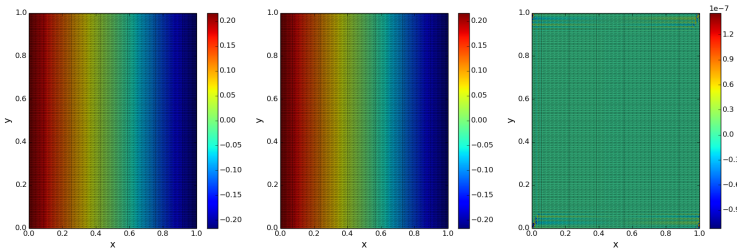


**Figure 4.2:** Left: Explicit solution  $u$ . Center: Numerical solution  $u_{128}$ . Right:  $u - u_{128}$ .

As seen the numerically computed solution is almost identical to the true. The errors are:

$$\frac{\|u - u_{128}\|_{L^2}}{\|u\|_{L^2}} = 5.2 \cdot 10^{-8} \quad \text{and} \quad \frac{\|u - u_{128}\|_{H^1}}{\|u\|_{H^1}} = 6.3 \cdot 10^{-6} \quad (4.14)$$

and on the electrodes

$$\frac{|U - U_{128}|}{|U|} = 3.7 \cdot 10^{-14} \quad (4.15)$$

This is a very good indicator for the correctness of the forward solver. Notice that the largest errors occur around the endpoints of the electrodes, especially near  $(0, 0)$  and  $(0, 1)$ , whereas the error elsewhere are very close to zero.

Similar results are seen when using the electrodes (4.7) and (4.8).

Assuming the forward solver works as intended, we will now focus on more complex scenarios. In these scenarios we do not have an explicit formula for the solution of the forward problem. Therefore we will throughout this chapter consider a solution produced on a very fine mesh as the true solution,  $u = u_{1024}$ .

### 4.3 Experiments with smooth conductivity

In this section we let the conductivity  $\sigma$  be smooth on  $\Omega$  given by the Gaussian function

$$\sigma(x, y) = 10e^{-\left(\frac{(x-0.3)^2}{0.1} + \frac{(y-0.4)^2}{0.1}\right)} + 0.6 \quad (4.16)$$

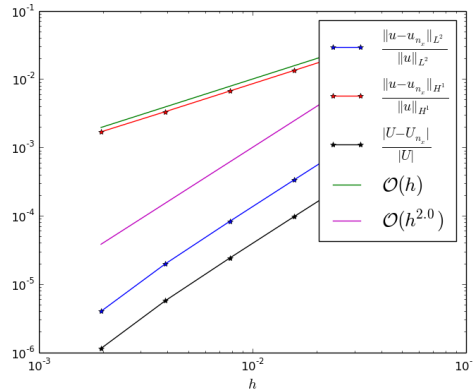


**Figure 4.3:** Convergence rate w.r.t. elementsize  $h$ . Here with conductivity given in (4.16) and electrodes defined in (4.5)- (4.6)

We start by using the electrodes (4.5) and (4.6). In Figure 4.3 is a plot of the convergence rate, w.r.t. the element size  $h$ . This is defined as  $h := n_x^{-1}$ . The error of  $u_{n_x}$  in  $H^1$  has a convergence of an order very close to 1, exactly 0.98, whereas the convergence order in  $L^2$  and on the electrodes are larger than 2, exactly 2.3.

In Figure 4.4 is a plot of the convergence rate for two different combinations of the electrodes given in (4.9)-(4.12).

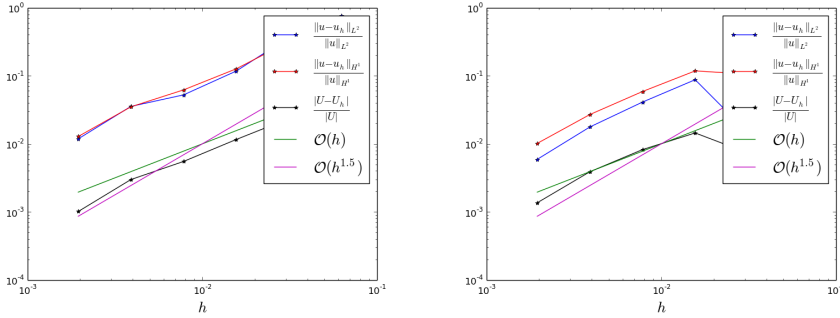


**Figure 4.4:** Convergence rate w.r.t. elementsize  $h$ . Here with conductivity given in (4.16) and to the left with two electrodes defined in (4.9) and (4.10), and to the right with the electrodes (4.9)- (4.12)

Here we see almost same order of convergence in both scenarios. There are some difference for large values of  $h$ , but for small values it looks the same. In  $L^2$  and  $H^1$  the error of  $u_{n_x}$  have an order between 1 and 1.5. In the scenario with two electrodes (to the left) the order is 1.07 and 1.13 for  $L^2$  and  $H^1$  respectively, whereas the similar orders in the scenario with four electrodes (to the right) are 1.40 and 1.27. Regarding the error on the electrodes the orders are measured to be 1.22 in the case with two electrodes and 1.30 in the case with four electrodes.

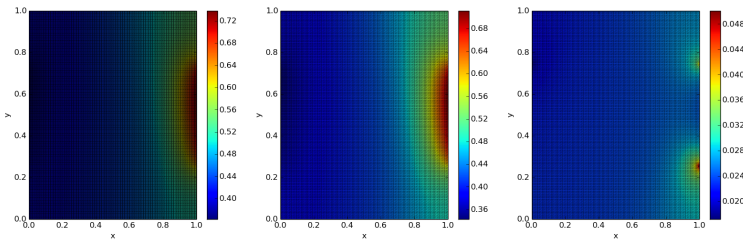


**Figure 4.5:** Left:  $u$ . Center:  $u_{128}$ . Right:  $u - u_{128}$ . Here with conductivity given in (4.16) and with two electrodes defined in (4.9) and (4.10).

The errors are here in general also larger than the errors in the scenario shown in Figure 4.3. This could be explained by the fact that the errors occur around the endpoints of the electrodes. When we consider the electrodes (4.9)-(4.12) we introduce singularities at the endpoints of these electrodes. But we still have the singularities at the corners of the domain as well. In Figure 4.5 is a plot of the difference between  $u$  and  $u_{128}$  in the scenario with (4.9) and (4.10) as

electrodes. Here we clearly see how the large errors occur around the endpoints of the electrodes. Another thing worth noticing is that the difference  $u - u_{128}$  is non-negative. This is probably since, when the current moves from the right to the left, the voltage decreases in the same direction. The function computed on the rough mesh will then start the decrease before the one on the fine mesh, thus the positive difference. This is also seen when computing the solution  $u_{256}$  as seen in Figure 4.6.

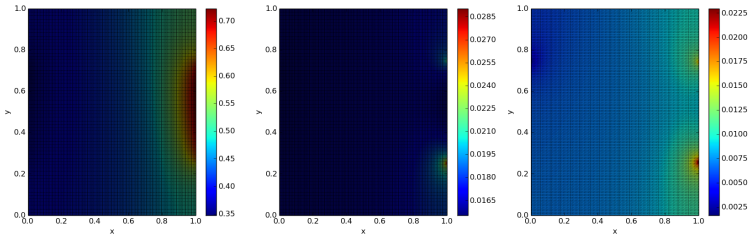


**Figure 4.6:** Left:  $u_{256}$ . Center:  $u - u_{256}$ . Right:  $u_{256} - u_{128}$ .

We see a clearly smaller error compared to the error of  $u_{128}$ . Again the difference  $u - u_{256}$  is positive, but with smaller values. Similar the difference  $u_{256} - u_{128}$  are also positive, which is again possibly because the function on the rough mesh starts decreasing faster. This could be since the solution in a sense is concave.

## 4.4 Experiments with piecewise constant conductivity

In this section we consider the problem, when the conductivity is discontinuous given by the piecewise constant function:

$$\sigma(x, y) = 1 + 5\chi_{B_{0.2}(0.7,0.7)}(x, y) + 10\chi_{B_{0.1}(0.2,0.2)}(x, y) \quad (4.17)$$

Here  $\chi_{B_r(x_0, y_0)}$  defines the characteristic function on the ball with radius  $r$  and center  $(x_0, y_0)$ . This conductivity is not in accordance with the theory where we required it to be differentiable continuous.

Using the same types of electrodes as in the previous sections we generate the convergence plot seen in Figures 4.7 and 4.8.

In the case of the two electrodes (4.5) and (4.6) showed in Figure 4.7 we see almost the same behaviour as in the case with smooth conductivity, although

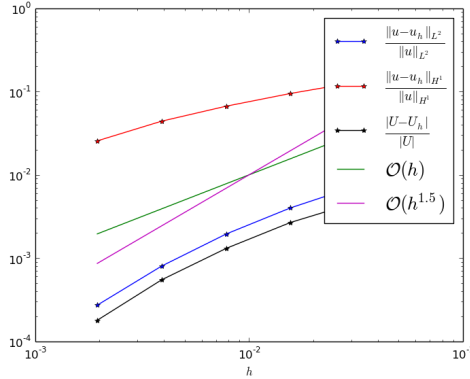


**Figure 4.7:** Convergence rate w.r.t. elementsize  $h$ . Conductivity is given in (4.17) and electrodes defined in (4.5)- (4.6)

the order of convergence is generally lower here. In  $L^2$  and on the electrodes the order is 1.4, whereas it was 2.3 with smooth conductivity, and in  $H^1$  it is of order 0.7, which was 0.98 with smooth conductivity.

In the second case we consider the electrodes (4.9) and (4.12). As seen in the left of Figure 4.8 there is a clear outlier in the case of the electrode error. Other than that it looks similar to the results of the previous section. There are although a small difference. For small values of  $h$  we see how the error in  $L^2$  starts converging faster than that of  $H^1$ , where we in the previous section saw same order of convergence. Here the orders are 1.7 and 0.9 for  $L^2$  and  $H^1$ , respectively, whereas it for the error on the electrodes are 1.5 (if we delete the outlying point). In general it is possible to see these outliers on the electrodes, especially when using the electrodes (4.9)-(4.12).

Finally in the case with four electrodes (4.9)-(4.12), we also see that the error of  $L^2$  has a higher order of convergence than that of  $H^1$ . The order of the error on the electrodes are similar to the one in  $L^2$ , which is 1.3. For the error in  $H^1$  the order is 0.97.

In Figure 4.9 is the solution to the forward problem  $u$ , the approximation  $u_{128}$  and their difference plotted in the scenario with the four electrodes (4.9)-(4.12). Notice again how the errors occur at the endpoints of the electrodes. Notice also how the voltage in the areas of high conductivity are almost constant. Furthermore we again see that the difference  $u - u_{128}$  is positive, and that in areas of large conductivity, this difference is almost constant. This can probably also explain why we see higher order of convergence in  $L^2$  than in  $H^1$ . If we look

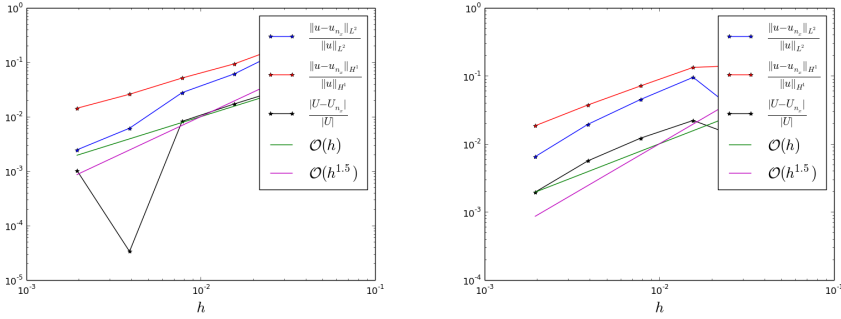


**Figure 4.8:** Convergence rate w.r.t. elementsize  $h$ . Here with conductivity (4.17). Left: The scenario with the electrodes (4.9) and (4.10). Right: With electrodes (4.9)-(4.12)

at the boundary of the balls with high conductivity we see that  $u-u_{128}$  has some small jumps. It is probably since these discontinuities are hard to approximate using more rough meshes. Hence it seems easier for the approximation  $u_{n,x}$  to capture the function values of the true solution, but a lot more difficult to capture the right values of the gradient.

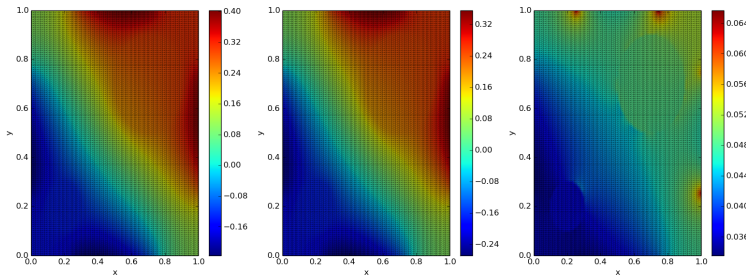


**Figure 4.9:** Left:  $u$ . Center: Solution  $u_{128}$ . Right:  $u - u_{128}$ . Computed with electrodes (4.9)-(4.12) and conductivity (4.17).

## 4.5 Conclusion on experiments

From the experiments where we have an explicit solution of the forward problem, we conclude that our solver seems to work fine.

For a relatively fine mesh, i.e. meshes of  $128 \times 128$  elements and larger, we

generally achieve a relative error in  $H^1$  ranging from 0.1% to 5%. In  $L^2$  the error is generally smaller and is in the range from  $5 \cdot 10^{-6}\%$  to 4%. The smallest errors are achieved when having a smooth conductivity. This seems reasonable since the theory only holds for conductivities in  $C^1$ . Although the theory applies to these conductivities it still seems to work in the case of having a discontinuous conductivity, although the errors are larger.

Throughout the experiments we have seen an order of convergence between 1 and 2.5. These results seems appropriate considering the results of [DS15]. Furthermore the errors seems largest around the endpoints of the electrodes, which is also consistent with [DS15]. Thus too achieve smaller errors it would be a good idea to have a very fine mesh around the endpoints of the electrodes. Notice also that the largest errors actually occur at electrodes from where the current are injected. Thus an even finer mesh here would be a good idea.

Regarding the solutions of the forward problems, the voltage  $u$  is largest close to the electrodes where the current are injected and smallest in close range of the electrodes where a current is extracted. In areas of large conductivity the voltage is almost constant, and the larger conductivity, the more constant is the voltage.

Finally it seems that the value of the voltage in the domain is increasing when the mesh is getting finer.



# Reconstructing conductivity

---

In Chapter 3 we discussed the non-uniqueness of the inverse problem. But we also discussed how knowledge of  $a = \sigma|\nabla u|$  and  $u$  on  $\Upsilon := \Gamma \cup \bigcup_{k=1}^N e_k$ , with  $\Gamma$  being a curve connecting the electrodes, makes it possible to reconstruct  $\sigma$ . Therefore we will in this chapter assume knowledge of  $a = \sigma|\nabla u|$  and  $u(\Upsilon)$ .

In this chapter we call  $(\sigma, u)$  a pair if  $(u, U)$  is the solution to the forward problem with conductivity  $\sigma$ . The idea would now be to find a pair  $(\tilde{\sigma}, \tilde{u})$  that satisfies  $\tilde{\sigma}|\nabla \tilde{u}| = a$ . Once we have such a pair we will use the information in  $u(\Upsilon)$  to relate  $(\sigma, u)$  and  $(\tilde{\sigma}, \tilde{u})$ .

## 5.1 Algorithm for reconstruction

In this section we construct an algorithm, which finds a pair  $(\tilde{\sigma}, \tilde{u})$ , s.t.  $\tilde{\sigma}|\nabla \tilde{u}| = a$ . A way to do this is as follows.

1. Initial guess for the conductivity,  $\sigma_0$ , fx.  $\sigma_0 = 1$ .
2. Solve the forward problem with  $\sigma_0$  as conductivity. Call this solution  $(u_0, U_0)$ .

3. Define  $\sigma_1$  by

$$\sigma_1(x, y) = \frac{a}{|\nabla u_0|} \quad (5.1)$$

4. Given conductivity  $\sigma_n$  compute  $(u_n, U_n)$  by solving the forward problem.

5. Is  $\|a - \sigma_n |\nabla u_n|\|_{L^2} < \textit{tolerance}$ ? If yes, we have a pair  $(\sigma_n, u_n)$ . If no, proceed to 6.

6. Given  $u_n$  compute  $\sigma_{n+1}$  by

$$\sigma_{n+1}(x, y) = \frac{a}{|\nabla u_n|} \quad (5.2)$$

and repeat 4.

The idea behind the sixth step is to ensure that  $\sigma_{n+1} |\nabla u_n| = a$ . Notice that there is a problem in constructing the conductivity if there are points where  $\nabla u_n = 0$ . In these situations we define an  $\epsilon \ll 1$  s.t. if there is a point  $(x_0, y_0)$  where  $\frac{a}{|\nabla u_n|}(x_0, y_0) > \epsilon^{-1}$ , we let  $\sigma_{n+1}(x_0, y_0) = \epsilon^{-1}$ . In the experiments this is only seen very few times. We choose  $\epsilon$  very small, s.t. we ensure that  $\sigma_{n+1} |\nabla u_n| = a$ .

In the next we will show how the sequence produced in the algorithm are a decreasing sequence with respect to  $G_a$  (3.1). This is proved in the lemma below.

**LEMMA 5.1** *Assume  $\tilde{u} \in H^1(\Omega)$  and there is an  $\epsilon > 0$  s.t.*

$$\epsilon \leq \frac{a}{|\nabla \tilde{u}|} \leq \frac{1}{\epsilon}. \quad (5.3)$$

*Let  $\sigma = \frac{a}{|\nabla u|}$  and let  $(u, U)$  be the unique solution of the forward problem with conductivity  $\sigma$ . Then*

$$G_a(u, U) \leq G_a(\tilde{u}, \tilde{U}) \quad \text{for any } \tilde{U} \text{ satisfying } \sum_{k=1}^N \tilde{U}_k = 0, \quad (5.4)$$

and if  $G_a(u, U) = G_a(\tilde{u}, \tilde{U})$ , then  $(u, U) = (\tilde{u}, \tilde{U})$ .

PROOF. Choose  $\tilde{U}$ , s.t.  $\sum_{k=1}^N \tilde{U}_k = 0$ . Then

$$G_a(\tilde{u}, \tilde{U}) = \int_{\Omega} a|\nabla\tilde{u}|dx + \sum_{k=1}^N \int_{e_k} \frac{1}{2z_k} (\tilde{u} - \tilde{U}_k)^2 ds - \sum_{k=1}^N I_k \tilde{U}_k \quad (5.5)$$

$$= \int_{\Omega} a|\nabla\tilde{u}|dx + \frac{1}{2} \sum_{k=1}^N \int_{e_k} \frac{1}{z_k} (\tilde{u} - \tilde{U}_k)^2 ds - \sum_{k=1}^N I_k \tilde{U}_k \quad (5.6)$$

$$= \frac{1}{2} \int_{\Omega} a|\nabla\tilde{u}|dx + F_{\sigma}(\tilde{u}, \tilde{U}). \quad (5.7)$$

By Theorem 2.10,  $(u, U)$  is a minimizer of  $F_{\sigma}(u, U)$ . Thus

$$G_a(\tilde{u}, \tilde{U}) = \frac{1}{2} \int_{\Omega} a|\nabla\tilde{u}|dx + F_{\sigma}(\tilde{u}, \tilde{U}) \geq \frac{1}{2} \int_{\Omega} a|\nabla\tilde{u}|dx + F_{\sigma}(u, U). \quad (5.8)$$

Next

$$G_a(u, U) = \int_{\Omega} a|\nabla u|dx + \frac{1}{2} \sum_{k=1}^N \int_{e_k} \frac{1}{z_k} (u - U_k)^2 ds - \sum_{k=1}^N I_k U_k \quad (5.9)$$

$$\leq \frac{1}{2} \int_{\Omega} \frac{a}{|\nabla\tilde{u}|} |\nabla u|^2 dx + \frac{1}{2} \int_{\Omega} a|\nabla\tilde{u}|dx \quad (5.10)$$

$$+ \frac{1}{2} \sum_{k=1}^N \int_{e_k} \frac{1}{z_k} (u - U_k)^2 ds - \sum_{k=1}^N I_k U_k$$

$$= \frac{1}{2} \int_{\Omega} a|\nabla\tilde{u}|dx + F_{\sigma}(u, U). \quad (5.11)$$

Here the inequality in (5.10) comes by Cauchy-Schwarz and the fact that  $\sqrt{ab} \leq \frac{1}{2}a + \frac{1}{2}b$ :

$$\int_{\Omega} a|\nabla u|dx = \int_{\Omega} \left( \frac{a}{|\nabla u|} \right)^{1/2} |\nabla\tilde{u}| \left( \frac{a}{|\nabla\tilde{u}|} \right)^{1/2} |\nabla u|dx \quad (5.12)$$

$$\leq \left( \int_{\Omega} a|\nabla\tilde{u}|dx \right)^{1/2} \left( \int_{\Omega} \frac{a}{|\nabla\tilde{u}|} |\nabla u|^2 dx \right)^{1/2} \quad (5.13)$$

$$\leq \frac{1}{2} \int_{\Omega} \frac{a}{|\nabla\tilde{u}|} |\nabla u|^2 dx + \frac{1}{2} \int_{\Omega} a|\nabla\tilde{u}|dx. \quad (5.14)$$

Hence

$$G_a(u, U) \leq \frac{1}{2} \int_{\Omega} a|\nabla\tilde{u}|dx + F_{\sigma}(u, U) \leq G_a(\tilde{u}, \tilde{U}), \quad (5.15)$$

for all  $\tilde{U}$  satisfying  $\sum_{k=1}^N \tilde{U}_k = 0$ . Furthermore if we have equality in (5.4), we have equality in (5.8), thus  $F_{\sigma}(\tilde{u}, \tilde{U}) = F_{\sigma}(u, U)$ . Since  $(u, U)$  is a solution

to the forward problem, with conductivity  $\sigma$ , it is by Theorem 2.10 a unique minimizer of  $F_\sigma$ , thus  $(u, U) = (\tilde{u}, \tilde{U})$ .  $\square$

So the the sequence generated by the algorithm above is decreasing w.r.t.  $G_a$ . This although does not mean, that the sequence finds the true pair  $(u, \sigma)$ , since by Proposition 3.1, there is no unique minimizer of  $G_a$ .

## 5.2 Generating $\phi$

Assume we know both  $u$  and  $\tilde{u}$  on  $\Upsilon$ . By Proposition 3.4 the ranges of  $\tilde{u}(\overline{\Omega})$  and  $u(\overline{\Omega})$  equals the ranges of  $\tilde{u}(\Upsilon)$  and  $u(\Upsilon)$ , respectively. As shown in Theorem 3.2,  $\phi$  maps from  $\tilde{u}(\overline{\Omega})$  to  $u(\overline{\Omega})$ . Hence knowledge of  $u$  and  $\tilde{u}$  on  $\Upsilon$  combined with the fact that  $u$  and  $\tilde{u}$  are continuous on  $\overline{\Omega}$ , thus also on  $\Upsilon$ , gives us knowledge of the entire interval on which  $\phi$  is defined, as well as the entire range of  $\phi$ .

In practice we only know  $u$  and  $\tilde{u}$  in a finite number of points on  $\Upsilon$ . Assume we know the values in the points  $\{x_i\}$  and call these values  $\{u_i\}$  and  $\{\tilde{u}_i\}$ . Assume these sequences are sorted. Knowing the values in these points we can approximate  $\phi$ . This is done by a linear interpolation between these points. Thus if we want to compute  $\phi(k)$  for some  $k$ , we find  $j$  s.t.  $\tilde{u}_{j-1} \leq k \leq \tilde{u}_j$ . Then we define  $\phi(k)$  by:

$$\alpha = \frac{u_j - u_{j-1}}{\tilde{u}_j - \tilde{u}_{j-1}} \quad (5.16)$$

$$\phi(k) = \alpha(k - \tilde{u}_j) + u_j \quad (5.17)$$

An example of this can be seen in the left of Figure 5.3.

The construction of  $\phi'$  can be done in multiple ways. One way is just to differentiate the  $\phi$  found above. Then  $\phi'$  will be piecewise constant. The more points on  $\Upsilon$  in which we know the values of  $\tilde{u}$  and  $u$ , the more precise should this approximation be. There are although also cons by having knowledge in a large number of points. Assuming that in two close points, the differences  $\tilde{u}_j - \tilde{u}_{j-1}$  and  $u_j - u_{j-1}$  are of size  $10^{-1}$  and  $10^{-4}$ , respectively. This will lead to a value of  $\phi'$  at around  $10^{-3}$ . Hence when reconstructing  $\sigma$  by use of  $(\phi')^{-1}$ , we get a very high value of  $\sigma$ . This is a quite bad situation.

There are two ways to avoid this scenario. One way is two simply just to avoid the information given in one point, if the difference in  $u$  compared to the

difference in  $\tilde{u}$  are very small or very large. Another way is to calculate the derivative by using values of  $u$  and  $\tilde{u}$  in more than two points. Say we want to determine the derivative of  $\phi$  at a value  $v$  between  $\tilde{u}_{j-1}$  and  $\tilde{u}_j$ . Then the simplest way to calculate  $\phi'(v)$ , as describe, is

$$\phi'(v) = \frac{u_j - u_{j-1}}{\tilde{u}_j - \tilde{u}_{j-1}}. \quad (5.18)$$

This could as mentioned earlier be critical if the denominator is a lot smaller or bigger than the numerator. Instead of avoiding these points we can consider the values of their neighbours. Some different ways of calculating  $\phi'(v)$  is then:

$$\phi'(v) = \frac{u_{j+1} - u_{j-2}}{\tilde{u}_{j+1} - \tilde{u}_{j-2}} \quad (5.19)$$

$$\phi'(v) = \frac{1}{4} \left( \frac{u_{j-1} - u_{j-2}}{\tilde{u}_{j-1} - \tilde{u}_{j-2}} + 2 \frac{u_j - u_{j-1}}{\tilde{u}_j - \tilde{u}_{j-1}} + \frac{u_{j+1} - u_j}{\tilde{u}_{j+1} - \tilde{u}_j} \right). \quad (5.20)$$

There are pros and cons for any choice of method. The method in (5.18) are in principle the correct way, since we here use all the exact known values. On the other hand the solution computed through the algorithm only approximately satisfy that  $\tilde{\sigma}|\nabla\tilde{u}| = a$  and therefore there could be some outliers, which can interfere with our computation of  $\phi'$ . Another thing to have in mind is that the number of points on the boundary where we know  $u$  and  $\tilde{u}$  depends on the choice of our mesh, and how fine it is.

In general the method which we will use is the one given in (5.18), but where we avoid outliers. The question is then how to define, when a point is an outlier. We will consider it an outlier if the measured derivative are below  $10^{-3}$  or above  $10^3$ .

## 5.3 Reconstruction with smooth conductivity

In this section we consider, how the reconstruction works, when the true conductivity is defined by a smooth function. Let us consider the conductivity given in (4.16).

Let (4.9) and (4.10) be the electrodes. As seen in the experiments of the forward problem, choosing a mesh at size  $128 \times 128$  would give us an error ( on  $u$  in  $L^2$  and  $H^1$ ) of the solution of the forward problem at around 1% – 2%. We define the curve  $\Gamma$  connecting the electrodes by

$$\Gamma = \{(x, y) | (y = 1 \text{ and } 0 \leq x \leq 1) \text{ or } (0.75 < y < 1 \text{ and } (x = 0 \text{ or } x = 1))\}. \quad (5.21)$$

First let us compute  $a$ . A plot of  $\sigma$ , the solution to the forward problem  $u$  and  $a$  can be seen in Figure 5.1. Notice here how the largest values of  $a$  are near the electrodes and especially near the endpoints of the electrodes.

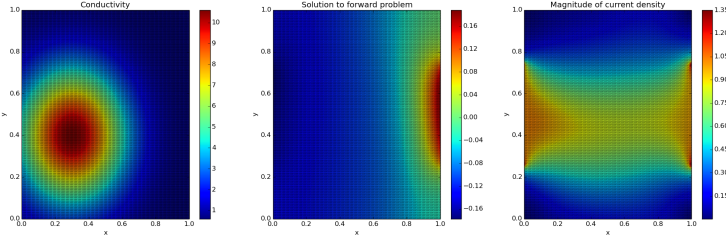


**Figure 5.1:** Left: The conductivity. Center: Solution to the forward problem. Right: Magnitude of the current density,  $a = \sigma|\nabla u|$ .

For the reconstruction we will choose a tolerance for when to stop the algorithm. An ideal thing is if this tolerance depends on  $a$ , such that the error becomes relative. Let us therefore choose the tolerance to be  $\|a\|_{L^2} \cdot 10^{-3}$ .

In Figure 5.2 is a plot of the pair  $(\tilde{\sigma}, \tilde{u})$  achieved through the algorithm, as well as  $\tilde{a} = \tilde{\sigma}|\nabla \tilde{u}|$ .

Notice how the conductivity  $\tilde{\sigma}$  seems relative far from the true conductivity. The computed  $\tilde{u}$  have a similar structure as  $u$  but not quite the same. Finally the difference between  $a$  and  $\tilde{a}$  are very small, with only a few differences around the endpoints of the electrodes. Thus the algorithm does not find the true conductivity  $\sigma$ , but a pair  $(\tilde{\sigma}, \tilde{u})$  s.t.  $\tilde{\sigma}|\nabla \tilde{u}| \approx a$ . By knowledge of  $u$  on  $\Upsilon$  we generate the  $\phi$ -function as described in the previous section. In Figure 5.3 is a plot of  $\phi$  and  $(\phi')^{-1}$ .

Notice how  $\phi$  seems smooth, but a look at  $(\phi')^{-1}$  shows that this is not the case. Also notice how  $\phi$  is increasing. When constructing  $(\phi')^{-1}$  we have in this case used the method in (5.20), but also avoiding some points if they were to close to each other.

Next we compute an estimation for the solution to the forward problem  $u$ . In Figure 5.4 is a plot of  $u^* = \phi(\tilde{u})$  and the difference  $u - u^*$ .

As seen  $u$  and  $u^*$  are almost the same, only with some errors around the one electrode. The relative errors in this scenario are

$$\frac{\|u - u^*\|_{L^2}}{\|u\|_{L^2}} = 0.002 \quad \text{and} \quad \frac{\|u - u^*\|_{H^1}}{\|u\|_{H^1}} = 0.03. \quad (5.22)$$

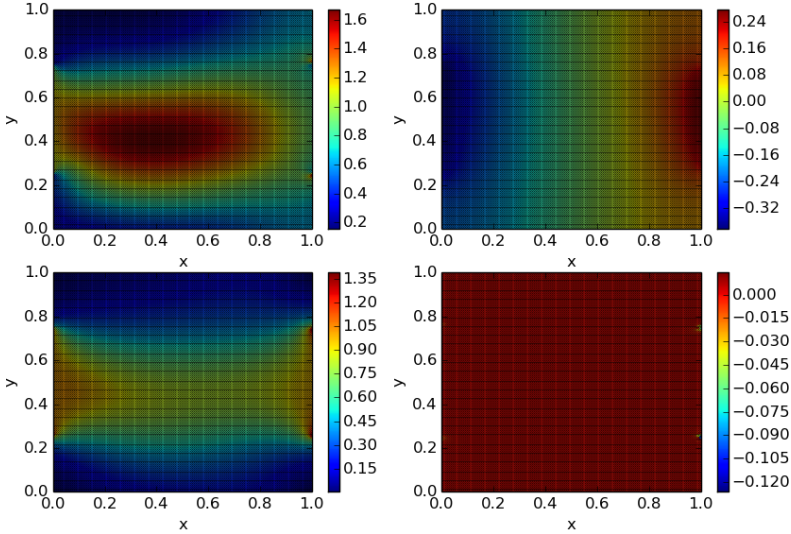


**Figure 5.2:** Upper left: Conductivity  $\tilde{\sigma}$  after algorithm finished. Upper right: Solution of forward problem  $\tilde{u}$ . Lower left:  $\tilde{a} = \tilde{\sigma}|\nabla\tilde{u}|$ . Lower right:  $\tilde{a} - a$ .

We are now ready to compute the conductivity. There are two ways of computing this. The first one is simply by use of the  $\phi$  and Theorem 3.2 and the second is by knowledge of  $a$  and  $u^*$ :

$$\sigma^* = (\phi'(\tilde{u}))^{-1}\tilde{\sigma} \quad \text{and} \quad \sigma_2^* = \frac{a}{|\nabla u^*|}. \quad (5.23)$$

In Figure 5.5 is a plot of the two computed conductivities as well as their errors. Both estimations seems quite good. As seen in both cases, the errors appear around the electrodes. There are although a difference in the type of error. For  $\sigma^*$  the errors are seems to be single points. For  $\sigma_2^*$  the errors are more curved shapes around the electrodes. Notice also how there seems to be some wave like errors, in the middle of the domain, especially at  $\sigma^*$ . This seems to happen when the true conductivity increases faster. The current will here move towards the places with large conductivity. The errors might come because the reconstruction algorithm capture these movements a bit later than they actually happen. The errors are:

$$\frac{\|\sigma - \sigma^*\|_{L^2}}{\|\sigma\|_{L^2}} = 0.047 \quad \text{and} \quad \frac{\|\sigma - \sigma_2^*\|_{L^2}}{\|\sigma\|_{L^2}} = 0.005. \quad (5.24)$$

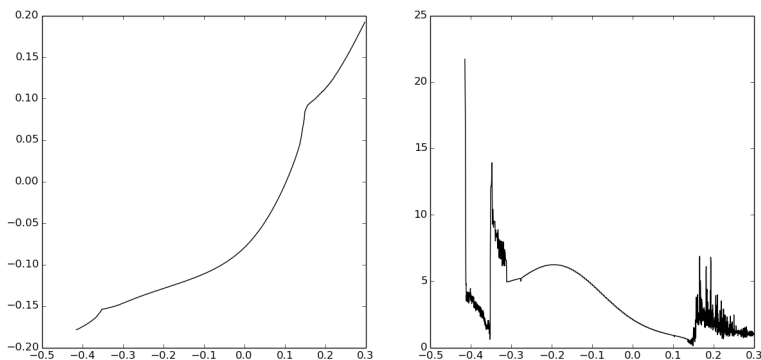


Figure 5.3: Left:  $\phi$ . Right:  $(\phi')^{-1}$ .

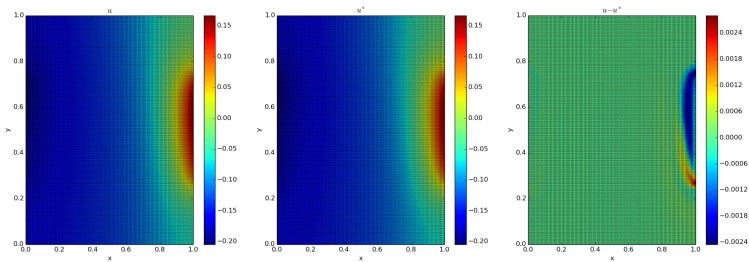
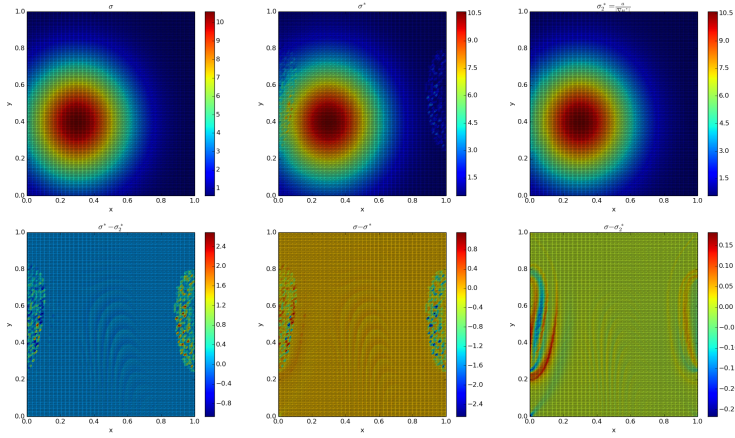


Figure 5.4: Left: Solution  $u$ . Center: Solution through reconstruction  $u^*$ . Right:  $u - u^*$ . This is in the case with smooth conductivity (4.16) and electrodes (4.9) and (4.10).

As seen the error on  $\sigma_2^*$  are nearly ten times smaller. But in both cases we get a nice small error.

So this seems to work very well in the case with two electrodes. Further experiments show similar results for other choices of electrodes.





**Figure 5.5:** Upper left:  $\sigma$ . Upper center:  $\sigma^*$ . Upper right:  $\sigma_2^*$ . Lower left:  $\sigma^* - \sigma_2^*$ . Lower center:  $\sigma - \sigma^*$ . Lower right:  $\sigma - \sigma_2^*$ . This is in the case with smooth conductivity (4.16) and electrodes (4.9) and (4.10)

## 5.4 Reconstruction with piecewise constant conductivity

In this section we consider the case with a piecewise constant conductivity given as

$$\sigma(x, y) = 1 + 5\chi_{B_{0.2}(0.6, 0.6)}(x, y). \quad (5.25)$$

First let us consider a case with electrodes (4.5) and (4.6). In Figure 5.6 is a plot of the conductivity, solution of forward problem and  $a$ .

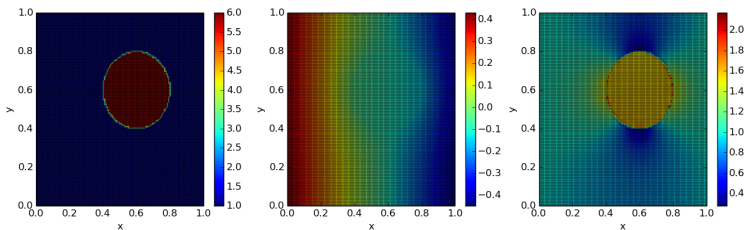


**Figure 5.6:** Left:  $\sigma$ . Center:  $u$ . Right:  $a = \sigma|\nabla u|$ .

Notice how the discontinuous conductivity clearly also make  $a$  discontinuous.

After running the algorithm we get the pair  $(\tilde{\sigma}, \tilde{u})$  plotted in Figure 5.7, together with the plot of  $\tilde{a}$ . The shape of the conductivity is captured, but the values are way different from the original. At the edge of the ball,  $\tilde{\sigma}$  has large values of size 900. This shows the difficulties of capturing the discontinuities. On the other hand the difference between  $a$  and  $\tilde{a}$  are very small, which essentially is what we want. The errors of  $\tilde{a}$  happens around the discontinuities of  $\sigma$ . Notice also that the error seems to happen at the discontinuities which points in the direction of the electrodes. The relative error of  $\tilde{a}$  are here:

$$\frac{\|a - \tilde{a}\|_{L^2}}{\|a\|_{L^2}} = 0.008. \quad (5.26)$$

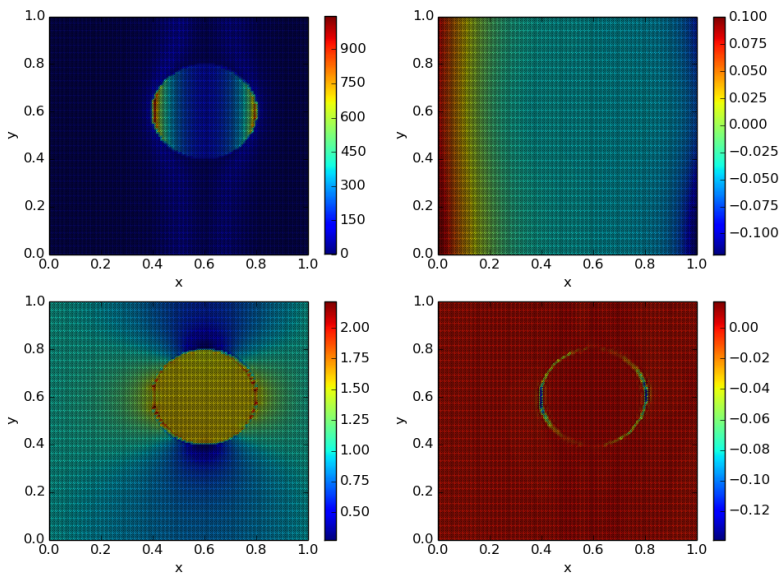


**Figure 5.7:** Upper left: Conductivity  $\tilde{\sigma}$  after algorithm finished. Upper center: Solution of forward problem  $\tilde{u}$ . Upper right:  $\tilde{a} = \tilde{\sigma}|\nabla\tilde{u}|$ . Lower left:  $\sigma - \tilde{\sigma}$ . Lower center:  $\tilde{u} - u$ . Lower right:  $\frac{\tilde{a}-a}{a}$ .

Next we construct the function  $\phi$  and its derivatives inverse. The derivative of  $\phi$  is in this case computed by (5.18). A plot of this can be seen in Figure 5.8.

Using this we are ready to reconstruct the conductivity. First using  $\phi$  we compute the voltage  $u^*$ . This is seen in Figure 5.9.

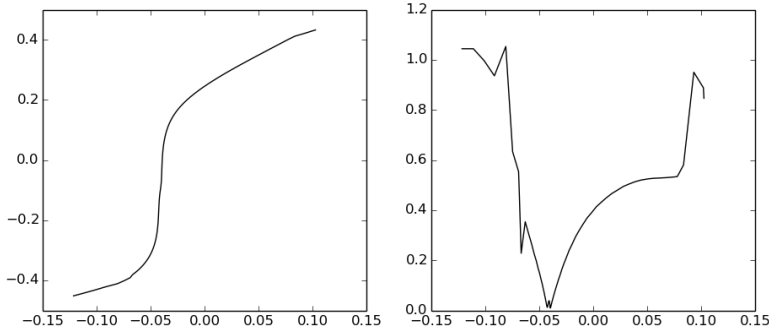


**Figure 5.8:** Left:  $\phi$ . Right:  $(\phi')^{-1}$ .

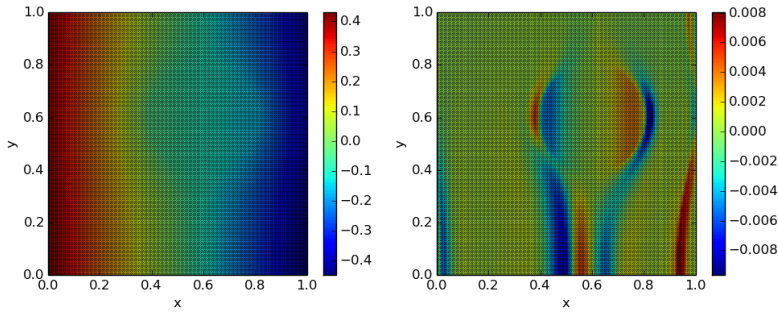


**Figure 5.9:** Left: The reconstruction  $u^*$ . Right:  $u - u^*$ .

The reconstruction seems to work quite well. The errors are:

$$\frac{\|u - u^*\|_{L^2}}{\|u\|_{L^2}} = 0.009 \quad \text{and} \quad \frac{\|u - u^*\|_{H^1}}{\|u\|_{H^1}} = 0.10. \quad (5.27)$$

The error of  $u^*$  in  $L^2$  is quite good. The error in  $H^1$  is larger. And this is also the error which affect the reconstruction of the conductivity. It is also worthwhile noticing the error of  $u^*$  in the off-centered ball with high conductivity. The error seems to be affine here, thus the difference of the gradients of  $u$  and  $\tilde{u}$  are constant. This will clearly affect the computation of the conductivity when using the method of  $\sigma_2^*$  in (5.23). In Figure 5.10 is a plot of the computed conductivities as well as the errors.

The computed  $\sigma^*$  seems as a good estimate of  $\sigma$ . As seen the form of the off-

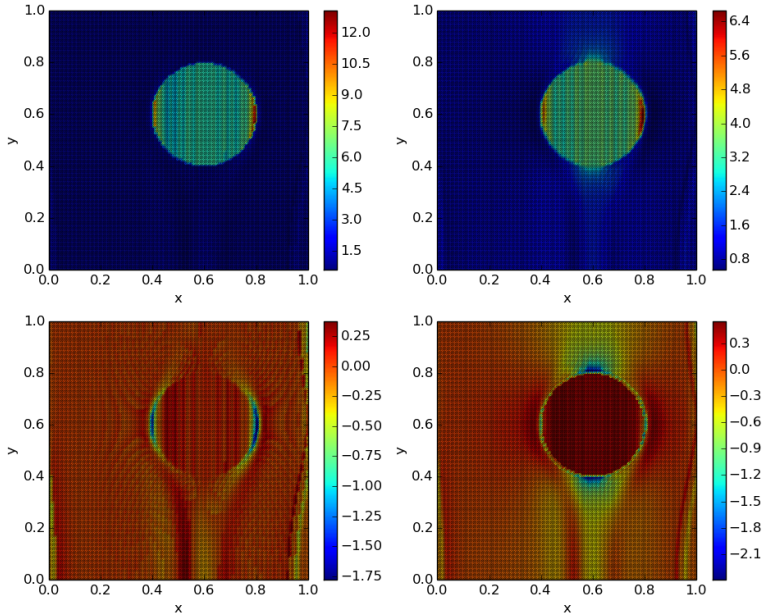


**Figure 5.10:** Upper left:  $\sigma^*$ . Upper right:  $\sigma_2^*$ . Lower left:  $\frac{\sigma - \sigma^*}{\sigma}$ . Lower right:  $\frac{\sigma - \sigma_2^*}{\sigma}$ .

centered ball is captured very well. There are although some large errors around the edge of the ball, especially at the edges pointing towards the electrodes. Notice also that  $\sigma_2^*$  captures the shape of the ball, but it does not capture the value. This is due to the discussion above of the error on  $u^*$ . At the ball it seems that  $\nabla u = c\nabla u^*$  for some constant  $c$ . So when computing  $\sigma_2^*$  the result will be

$$\sigma_2^* = \frac{a}{|\nabla u^*|} = \frac{a}{|c\nabla u|} = \frac{1}{|c|}\sigma, \quad (5.28)$$

Which explains why the error at the ball seems constant. The errors in this reconstruction are:

$$\frac{\|\sigma - \sigma^*\|_{L^2}}{\|\sigma\|_{L^2}} = 0.16 \quad \text{and} \quad \frac{\|\sigma - \sigma_2^*\|_{L^2}}{\|\sigma\|_{L^2}} = 0.4. \quad (5.29)$$

An error at 16% might seem large, but the shape and size of the conductivity are, as seen in the plots, captured quite well.

The errors appearing at the discontinuities could be decreased by doing the

reconstruction for multiple choices of electrodes, since they occur in the direction of the electrodes.

We will therefore in the next experiment consider the four electrodes (4.9)-(4.12), with a basis of the current pattern given by  $(I_1, I_2) = (-1.0, 1.0)$ ,  $(I_3, I_4) = (-1.0, 1.0)$  and  $(I_1, I_3) = (-1.0, 1.0)$ . We will do the reconstruction for all three choices and add them to one final reconstruction.

First let us consider the pattern  $(I_1, I_2) = (-1.0, 1.0)$ . A plot of the reconstructed conductivity is seen in Figure 5.11.

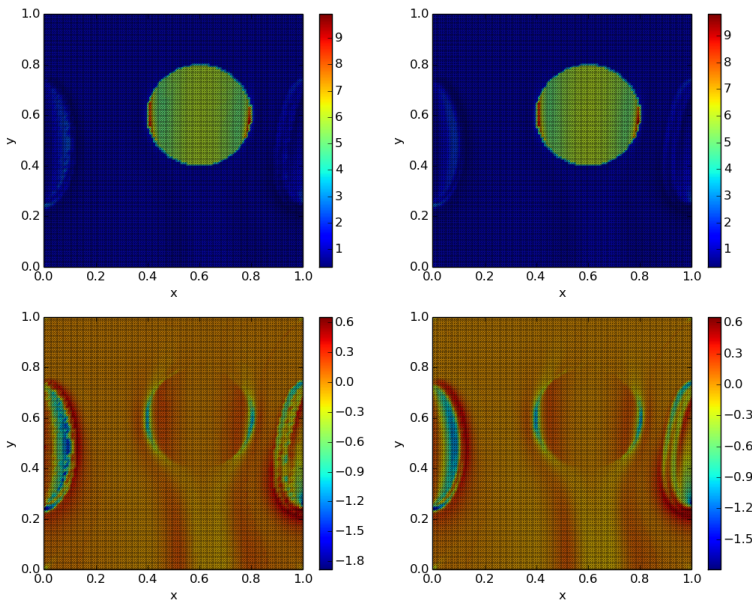


**Figure 5.11:** Upper left:  $\sigma^*$ . Upper right:  $\sigma_2^*$ . Lower left:  $\frac{\sigma - \sigma^*}{\sigma}$ . Lower right:  $\frac{\sigma - \sigma_2^*}{\sigma}$ .

It is here worth noticing how the errors are a combination of the errors found in the experiment with smooth conductivity shown in Figure 5.5, which appears near the electrodes and the errors in the previous example around the edge of the off-centered ball. The same is again seen if we use the current pattern  $(I_3, I_4) = (-1.0, 1.0)$  as seen in Figure 5.12.

Finally doing the reconstruction with the two electrodes (4.9) and (4.11) completes the results. This result can be seen in Figure 5.13. Notice that we see the



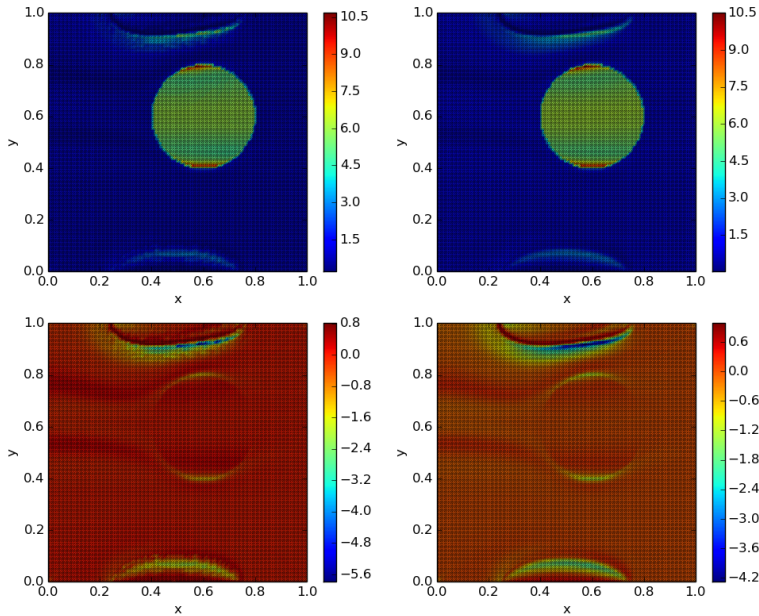


**Figure 5.12:** Upper left:  $\sigma^*$ . Upper right:  $\sigma_2^*$ . Lower left:  $\frac{\sigma - \sigma^*}{\sigma}$ . Lower right:  $\frac{\sigma - \sigma_2^*}{\sigma}$ .

same errors as before, but in this case the value inside the off-centered ball are not captured very well. One could explain this by the current travelling a short distance, and that the direct way between the electrodes does not go through the ball with high conductivity. Another thing to have in mind is that the scenario with these two electrodes requires less knowledge of  $u$  on the boundary compared to other choices of electrodes.

The average of the three previous computations are used as a final estimate of the conductivity. The two different computations  $\sigma^*$  and  $\sigma_2^*$  are almost equal through the experiments. Therefore we only consider the average of  $\sigma^*$ . This is seen in Figure 5.14. The relative error of the computed conductivity are here:

$$\frac{\|\sigma - \sigma^*\|_{L^2(\Omega)}}{\|\sigma\|_{L^2(\Omega)}} = 0.19. \quad (5.30)$$

This is not a small error, but the reconstruction captures the shape of the off-centered ball quite good. The value in the ball are a little less than the correct.

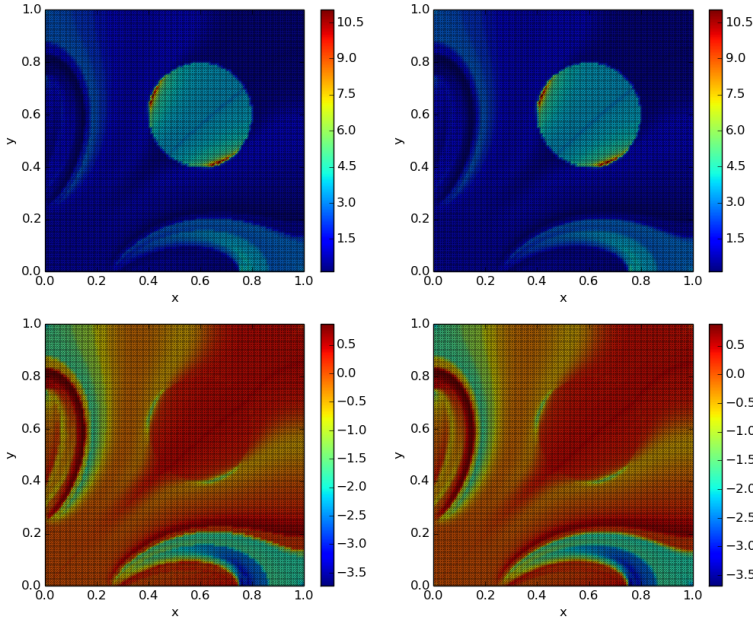


**Figure 5.13:** Upper left:  $\sigma^*$ . Upper right:  $\sigma_2^*$ . Lower left:  $\frac{\sigma - \sigma^*}{\sigma}$ . Lower right:  $\frac{\sigma - \sigma_2^*}{\sigma_2^*}$ .

Notice how errors still occur around all four electrodes, but they are decreased compared to the previous cases.

In real scenarios this method could be quite good since we do find the shape of the objects. There are although the question, if we then can identify the object correct, since we do not capture the exact conductivity of the object. Due to the fact that the conductivity varies a lot from tissue to tissue, the error we get might therefore be small enough to identify the object correctly. Another thing to have in mind is to think about what happens if objects occur very close to the electrodes. The fact of large errors occurring near the electrodes could make it impossible to identify these objects.

Finally it is worth mentioning that when we run the algorithm we cannot expect to get a decreasing sequence w.r.t.  $\|a - \tilde{a}\|_{L^2}$ . Since this is how we define the error, it could be, that if we choose the tolerance very low, the algorithm will never stop. Therefore we could apply another stop criteria, say after 1000 iterations. Generally in the cases of discontinuous conductivity one should not

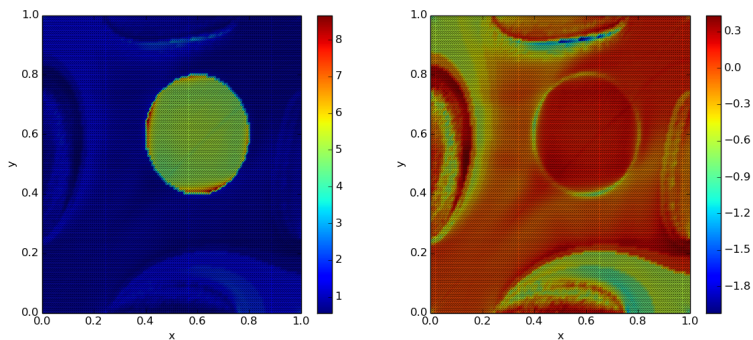


**Figure 5.14:** Left: Conductivity  $\sigma^*$  constructed as the average of multiple reconstructions. Right:  $\frac{\sigma - \sigma^*}{\sigma}$ .

expect the error  $\|a - \tilde{a}\|_{L^2}$  to be below 1% of  $\|a\|_{L^2}$ . What one could do is run the algorithm through a large number of iterations and pick out the pair which gives the smallest error on  $a$ . This is a bit intricately, but since the theory does not hold for discontinuous conductivity we cannot ensure that the algorithm will actually work.



# Conclusion and Perspective

---

Construction of our numerical solver shows that the inverse problem can be solved given some initial knowledge of the current density and voltage on the boundary. In cases of smooth conductivity we have seen errors around 5%, and for discontinuous conductivities between 15% and 20%, when the errors are measured in  $L^2$ . Although some will say these errors are large, the reconstruction clearly captures the shape of the objects. The exact conductivity at these objects may be a bit off, but generally they are close to the original. Smaller errors would probably be seen if using a finer mesh. Especially in the cases with smooth conductivity, since we in the investigation of the forward problem saw quite large orders of convergence with respect to the mesh size.

We have shown non-uniqueness of the inverse problem and shown that if two pairs  $(\sigma, u)$  and  $(\tilde{\sigma}, \tilde{u})$  satisfies  $\sigma|\nabla u| = \tilde{\sigma}|\nabla \tilde{u}|$ , then there exists a strictly increasing function  $\phi$ , defined on the range of  $\tilde{u}$ , s.t.  $\phi(\tilde{u}) = u$  and  $(\phi'(\tilde{u}))^{-1}\tilde{\sigma} = \sigma$ . Using the maximum principle we showed how one can construct  $\phi$  by knowledge of  $u$  and  $\tilde{u}$  on the boundary.

Through reconstruction we have seen how errors occur around the electrodes. This type of error was also identified when solving the forward problem. Here we saw how a fine mesh decreased these errors. For further reconstructions of the inverse problem it is worthwhile having these observations in mind and consider a very fine mesh around the electrodes. Furthermore we observed large errors

around discontinuities of the conductivity. These errors can be handled through a finer mesh, but as seen through computations of the forward problem, the order of decrease of the errors w.r.t. the mesh size is quite small if measured in  $H^1$ . Thus a finer mesh around discontinuities would maybe not provide a significantly smaller error, since the error in the inverse problem are related to the error in  $H^1$  of the forward problem. So for further reconstruction experiments it might not be worth having a very fine mesh around the discontinuities. Instead, since the errors mainly occurred at discontinuities facing the electrodes, a good idea is to reconstruct with multiple choices of the electrode set-up. This will decrease the errors around the discontinuities and also the errors around the electrodes.

We have used knowledge of the current density and of the voltage on the boundary. As mentioned in the introduction the current density can be achieved through MRI scans. Although the entire current density are available through these scans we only use the magnitude of it when reconstructing. One can think about if the current density could be used for more. Immediately Corollary 3.3 seems to answer this question, since equality of the magnitude implies equality of the entire current density. Regarding the knowledge of the voltage on the boundary, it is reasonable to believe that the voltage on the electrodes can be measured directly ([MS12]). But it is maybe not reasonable to believe we can get knowledge of the voltage on other parts of the boundary. By continuity of the voltage on the boundary, missing this information would imply that we are missing knowledge of  $\phi$  on one or more intervals of the range of  $\tilde{u}$ . This could in practice be handled by doing a linear interpolation on these intervals. Doing this it would be a good idea to have electrodes close to each other, since this will probably decrease the length of the unknown intervals.

## APPENDIX A

# Definitions, theorems, etc.

---

In this part of the Appendix we provide some extra notes and some of the theorems, definitions, propositions etc. used in the thesis. Some of the theorems are modified from where they originally was found, s.t. they fit to the cases in which we use them.

### A.1 Notes on traces, $H^{1/2}$ and $H^{-1/2}$

First let us consider how we can restrict  $u$  to the boundary  $\partial\Omega$ . As stated in the trace theorem, Theorem A.5, there exists a continuous mapping  $T_0 : H^1(\Omega) \rightarrow H^{1/2}(\partial\Omega)$ , s.t.  $T_0 u = u|_{\partial\Omega}$ . I will comment a bit more on this matter and how one should interpret  $H^{1/2}$ .

Assume  $u \in C(\bar{\Omega})$ . Then  $u$  can be restricted to the boundary by  $u|_{\partial\Omega} \in L^2(\partial\Omega)$  (Theorem A.3). Letting  $T_0$  be the operator restricting  $u$  to the boundary we get:

$$\|T_0 u\|_{L^2(\partial\Omega)} = \|u\|_{L^2(\partial\Omega)}. \quad (\text{A.1})$$

Furthermore, (Theorem A.3), there exists a constant  $C > 0$  s.t.

$$\|T_0 u\|_{L^2(\partial\Omega)} = \|u\|_{L^2(\partial\Omega)} \leq C \|u\|_{H^1(\Omega)}. \quad (\text{A.2})$$

Finally if  $u \in H^1(\Omega)$ , we can by density of  $C_c^\infty(\bar{\Omega})$  in  $H^1(\Omega)$  find a sequence in  $C_c^\infty(\bar{\Omega})$  converging to  $u$ . Letting the operator  $T_0$  act on this sequence and showing that the output is a Cauchy-sequence in  $L^2(\partial\Omega)$  finishes the argument, and we have that  $T_0$  maps from  $H^1(\Omega)$  into  $L^2(\partial\Omega)$ . It is not certain that  $T_0$  maps into the entire of  $L^2(\partial\Omega)$ , which gives raise to the definition of  $H^{1/2}(\partial\Omega)$ . We simply define it to be the range of the operator  $T_0$ ,  $H^{1/2}(\partial\Omega) = R(T_0)$ , thus  $H^{1/2}(\partial\Omega) \subset L^2(\partial\Omega)$ . We equip  $H^{1/2}(\partial\Omega)$  with the norm given by

$$\|\phi\|_{H^{1/2}(\partial\Omega)} = \min_{u \in H^1(\Omega), T_0 u = \phi} \|u\|_{H^1(\Omega)}. \quad (\text{A.3})$$

This also gives raise to the space  $H^{-1/2}(\partial\Omega)$  which will be defined as the dual space of  $H^{1/2}(\partial\Omega)$ , i.e.  $H^{-1/2}(\partial\Omega) = (H^{1/2}(\partial\Omega))'$ .

The space  $H^{-1/2}(\partial\Omega)$  will be helpful in the restriction of  $u$  to the boundary by  $\sigma \frac{\partial u}{\partial n}$ . We denote this operator  $T_1$ . First assume that  $u \in C^2(\Omega)$  and  $u$  solves the forward problem, i.e.  $\nabla \cdot \sigma \nabla u = 0$ . Using partial integration we then have

$$0 = \int_{\Omega} \nabla \cdot (\sigma \nabla u) \bar{v} \, dx = \int_{\partial\Omega} \sigma \frac{\partial u}{\partial n} \bar{v} \, ds - \int_{\Omega} \sigma \nabla u \cdot \nabla \bar{v} \, dx, \quad \forall v \in C^2(\Omega). \quad (\text{A.4})$$

So we the define  $\sigma \frac{\partial u}{\partial n} \in H^{-1/2}(\partial\Omega)$  by how it acts on a function  $v \in H^{1/2}(\partial\Omega)$ :

$$\left\langle \sigma \frac{\partial u}{\partial n}, v \right\rangle := \int_{\partial\Omega} \sigma \frac{\partial u}{\partial n} \bar{v} \, ds = \int_{\Omega} \sigma \nabla u \cdot \nabla \bar{v} \, dx. \quad (\text{A.5})$$

The integral  $\int_{\partial\Omega} \sigma \frac{\partial u}{\partial n} \bar{v} \, ds$  does not in itself make any sense at this point, but helps defining the operator.

Thus we now have an operator  $T_1 u = \sigma \frac{\partial u}{\partial n}$ . In [LM73] it is shown, that the mapping can be extended to hold for all  $u, v \in H^1(\Omega)$  and  $\nabla \cdot \sigma \nabla u \in L^2(\Omega)$ , s.t.  $T_1 : H^1(\Omega) \rightarrow H^{-1/2}(\partial\Omega)$ .

## A.2 Theorems, propositions, etc.

In some of the the theorems we consider the operator  $L$ , generally given by:

$$Lu = - \sum_{i,j} a^{ij} u_{x_i x_j} + \sum_i b^i u_{x_i} + cu \quad (\text{A.6})$$

In our cases  $Lu$  is defined by  $\nabla \cdot \sigma \nabla u$ , thus this will be the definition of  $Lu$  in this part of the Appendix.

**THEOREM A.1** (*Weak maximum principle*) Assume  $u \in C^2(\Omega) \cap C(\overline{\Omega})$  and

$$Lu = 0. \quad (\text{A.7})$$

Then  $u$  attains its maximum and minimum on  $\overline{\Omega}$  on  $\partial\Omega$ .

**Remark.** This theorem is stated in [Eva10], Theorem 1 pg. 344, where the proof is also found. It is used when establishing the maximum principle for the forward problem (Proposition 3.4).

**LEMMA A.2** (*Hopf's Lemma*) Assume  $u \in C^2(\Omega) \cap C^1(\overline{\Omega})$  and

$$Lu = 0. \quad (\text{A.8})$$

Assume there exists points  $x^M \in \partial\Omega$  and  $x^m \in \partial\Omega$  s.t.

$$u(x^M) > u(x) \quad \text{and} \quad u(x^m) < u(x) \quad \text{for all } x \in \Omega. \quad (\text{A.9})$$

Finally assume that there exists balls  $B_m$  and  $B_M$  such that  $B_m \subset \Omega$ ,  $B_M \subset \Omega$ ,  $x^m \in \partial B^m$  and  $x^M \in \partial B^M$ . Then

$$\frac{\partial u}{\partial n}(x^m) < 0 \quad \text{and} \quad \frac{\partial u}{\partial n}(x^M) > 0, \quad (\text{A.10})$$

where  $n$  is the out warded unit normal of  $B^m$  and  $B^M$ .

**Remark.** The proof of Lemma A.2 this is carried out in [Eva10] pg. 347-349. It is used when establishing the maximum principle for the forward problem (Proposition 3.4).

**THEOREM A.3** If  $\Omega$  is bounded with smooth boundary, then there exists a bounded linear operator

$$T : H^1(\Omega) \rightarrow L^2(\partial\Omega) \quad (\text{A.11})$$

such that

$$Tu = u|_{\partial\Omega} \quad \text{if } u \in H^1(\Omega) \cap C(\overline{\Omega})$$

and

$$\|Tu\|_{L^2(\partial\Omega)} = \|u\|_{L^2(\partial\Omega)} \leq C\|u\|_{H^1(\Omega)}$$

**Remark.** This is stated and proved in [Eva10] (pg. 272).

**THEOREM A.4** *Let  $\Omega$  be a  $C^{1,\alpha}$  domain and let  $L$  be a strictly elliptic operator. The if  $\phi \in C^{1,\alpha}(\overline{\Omega})$  and  $\sigma \in C^\alpha(\overline{\Omega})$ , the Dirichlet problem*

$$Lu = 0 \quad \text{in } \Omega, \quad u = \phi \quad \text{on } \partial\Omega \quad (\text{A.12})$$

*has a unique solution in  $C^{1,\alpha}(\overline{\Omega})$ .*

**Remark.** If  $\sigma \in C^\alpha(\Omega)$  instead, then the solution is in  $C^{1,\alpha}(\Omega)$ . We use this in Theorem 3.2. The proof can be found in [GT01] page 211.

**THEOREM A.5** (*Trace Theorem*) *Let  $\Omega$  be a smooth open set. Then for any  $s > \frac{1}{2}$  and multi index  $\alpha$ , s.t.  $s - \frac{1}{2} - |\alpha| > 0$ , the operator:*

$$\text{tr}^\alpha : H^s(\Omega) \rightarrow H^{s-|\alpha|-1/2}(\partial\Omega) \quad (\text{A.13})$$

$$u \rightarrow \partial^\alpha u|_{\partial\Omega} \quad (\text{A.14})$$

*is a continuous linear mapping.*

**Remark.** We use this theorem, when considering the trace operator in the proof of Proposition 2.1. We apply the theorem with  $s = 1$  and  $\alpha = 0$ . The proof can be found in [LM73] Lemma 7.2 pg. 32.

**THEOREM A.6** *Any bounded closed set of a Hilbert space is weakly compact*

**Remark.** This is a consequence of Banach-Alaoglu Theorem, which states that the closed unit ball of the dual space of a normed vector space is weakly compact, combined with Riesz Representation Theorem, which states that any Hilbert space is isomorphic with its dual.

**PROPOSITION A.7** *Let  $\Omega = [0, 1] \times [0, 1]$  and assume  $e_0$  and  $e_1$  defined by (4.5) and (4.6) are the only electrodes. If  $\sum_{k=1}^N U_k = 0$  and the conductivity  $\sigma$  is constant then the solution  $(u, U)$  of the forward problem is of the form*

$$u(x, y) = \alpha x + \beta, \quad (\text{A.15})$$

*where  $\alpha = -I_0\sigma^{-1}$  and  $\beta = \sigma(z_0 - z_1) + I_0\sigma^{-1}$ .*

**PROOF.** From Corollary 2.6 the problem has a unique solution. Thus assume the solution is given by  $u(x, y) = \alpha x + \beta$ . That  $u$  satisfies (1.1) and (1.3) does not affect the formula for  $\alpha$  and  $\beta$ .

We have that

$$\int_{e_0} \sigma \frac{\partial u}{\partial n} ds = -\alpha\sigma \quad \text{and} \quad \int_{e_1} \sigma \frac{\partial u}{\partial n} ds = \alpha\sigma. \quad (\text{A.16})$$

Thus if (1.4) is satisfied we must have  $\alpha = -I_0\sigma^{-1} = I_1\sigma^{-1}$ . Finally since  $u|_{e_0} = \beta$  and  $u|_{e_1} = \alpha + \beta$  we have that on  $e_0$ :

$$u + z_0\sigma \frac{\partial u}{\partial n} = \beta - z_0\sigma \quad (\text{A.17})$$

and on  $e_1$

$$u + z_1\sigma \frac{\partial u}{\partial n} = \beta + \alpha + z_1\sigma. \quad (\text{A.18})$$

So since (1.2) is satisfied and  $U_0 + U_1 = 0$  we have

$$0 = \beta - z_0\sigma + \beta + \alpha + z_1\sigma \quad \Leftrightarrow \quad \beta = \sigma(z_0 - z_1) + \alpha, \quad (\text{A.19})$$

and since  $\alpha = I_0\sigma^{-1}$  we are done.  $\square$





## APPENDIX B

# Pieces of code

---

In this part of the Appendix we will show some samples of the code that we use.

### B.1 Defining mesh, electrodes, function space etc.

In this section we show how to define the mesh and function spaces. When constructing the mesh, we use the build in function `UnitSquareMesh`, which defines a regular triangular mesh on the unit square:

```
nx = 128
ny = 128
mesh = UnitSquareMesh(nx,ny)
```

Next we can define the boundaries and electrodes of the mesh above. First we need to define the boundary of the mesh and how to mark the boundary. This is done by:

```
boundary_parts = MeshFunction("size_t", mesh, \
                             mesh.topology().dim()-1)
ds = Measure("ds", domain=mesh, subdomain_data=boundary_parts)
```

We mark the boundary by "ds". Now we can define the different boundary parts. If we want to define the left boundary of the domain, i.e. the electrode defined in (4.5), we do as follows.

```
class LeftBoundary(SubDomain):
    """ This class defines the left boundary, i.e. the
        boundary on the x[0]-axis of the domain."""
    def inside(self, x, on_boundary):
        tol = 1E-14
        # tolerance for coordinate comparisons
        return on_boundary and abs(x[0]) < tol
```

This class will return points on the boundary of the mesh, which satisfies that  $|x| < tol$ , where  $tol$  is given small tolerance. Due to computer uncertainty we can not write  $x[0]=0$ . In similar way we can define the right upper and left boundary. If we want to construct the electrode defined in (4.9) we can do this by:

```
class LeftBoundaryZeroFive(SubDomain):
    """ This class defines the middle of the left boundary,
        i.e. the boundary on the x[0]-axis of the domain,
        where  $0.25 < x[1] < 0.75$ ."""
    def inside(self, x, on_boundary):
        tol = 1E-14
        # tolerance for coordinate comparisons
        return on_boundary and abs(x[0]) < tol \
            and x[1] > 0.25 and x[1] < 0.75
```

Here we just require one more information compared to `LeftBoundary`, which is the bound on  $y$  ( $x[1]$ ). Similarly it can be done for the rest of the electrodes, (4.9)-(4.12). The rest part of the left boundary is now defined by:

```
class RestLeftBoundaryZeroFive(SubDomain):
    """ Defines the part of the boundary on the x-axis,
        which is not a part of the electrode. That is the
        points on the x-axis for where  $0.25 < x[1] < 0.75$ 
        is not true"""
    def inside(self,x,on_boundary):
        tol = 1E-14
        return on_boundary and abs(x[0]) < tol \
            and abs(x[1]-0.5) > 0.25
```

Finally the way we now mark the boundaries are done by:

```
Gamma_0 = LeftBoundary()
Gamma_0.mark(boundary_parts, 0)
```

Thus we can now call the left boundary by our mark `ds` and the number 0, i.e. `ds[0]`.

Next we construct the function space in which we seek a solution to the forward problem. There are two ways of constructing the function space depending on the method we use, described in Section 4.1. The first one is the one defined in (4.1) and (4.2).

```
N = 2 # Number of electrodes
# Defining function-space
H      = FunctionSpace(mesh, 'CG', 1)
RN     = VectorFunctionSpace(mesh, 'R', 0, N-1)
func_space = MixedFunctionSpace([H, RN])
```

First we need to define the number of electrodes. Then we construct the space `H`, which is the space for which we seek a solution of  $u$ . The `'CG'` means continuous Galerkin and the `'1'` is the order. Thus `H` consist of first order continuous Galerkin (Lagrange) functions defined on the mesh. Next we define `RN`, which is the function space for the vector  $U_N$ . It is real-valued `'R'` with order 0 and dimension `N-1`. The dimension is  $N - 1$  and not  $N$  due to the implementation as explained earlier.

Using the second method will not affect the definition of `H`. But it will change `RN` and furthermore we need to define a space for the helping constant  $c$ .

```
RN     = VectorFunctionSpace(mesh, 'R', 0, N)
C      = FunctionSpace(mesh, 'R', 0)
func_space = MixedFunctionSpace([H, RN, C])
```

What changes here is just that the dimension of `RN` is `N`. The function space for  $c$  is defined to be real and of order 0.

## B.2 Construction of conductivity

In the cases where the conductivity is a smooth function  $f(x)$ , it is easily defined by the use of `Expression`:

```
sigma = Expression("f(x)")
```

But it is a bit more difficult to construct a piecewise constant conductivity. In the class `CharacteristicFunctionDisk`. This class defines a function, which is 1 in the domain, except for in a ball centred at  $(x_0, y_0)$  with radius  $r$ , where the value is  $k$ .

```

class CharacteristicFunctionDisk(Expression):
    """ This class represents and manipulates
        a characteristic function of a disk centered
        at (x_center, y_center) of radius r. """
    def __init__(self, x_center, y_center, r, contrast_level):
        self.x_center = x_center
        self.y_center = y_center
        self.r = r
        self.contrast_level = contrast_level
        #super(Expression, self).__init__()

    def sqr_dist_to_center(self, x):
        return (x[0]-self.x_center)**2 \
               + (x[1]-self.y_center)**2

    def eval(self, value, x):
        if (self.sqr_dist_to_center(x) < self.r**2):
            value[0] = 1 + self.contrast_level
        else:
            value[0] = 1

```

### B.3 Solving the forward problem

In this section we show how the forward problem is solved, using the two methods described earlier. First we define the trial function ( $u, U$ ) and the test functions.

```

(u,U) = TrialFunctions(func_space)
(v,V) = TestFunctions(func_space)

```

Next we can construct the bilinear form  $B$  and the right hand side of the variational formulation. First we consider the case in (4.1) and (4.2). We use the command `grad` to define the gradient and `inner` to compute the dot product.

```

B = (inner(sigma*grad(u), grad(v)))*dx \
     + sum([1/z[i]*(u-U[i]) * (v - V[i]) \
            * ds(i) for i in range(N-1)]) \
     + (1/z[N-1]*(u+sum([U[i] for i in range(N-1)]))\
        *(v+sum([V[i] for i in range(N-1)])))*ds(N-1)

L = sum([I[i]*V[i]*dx for i in range(N-1)]) \
     + (I[N-1]*sum([-V[i] for i in range(N-1)]))*dx

```

Notice how the right hand side are defined by integrals  $\sum_{k=1}^{N-1} \int_{\Omega} I_k V_k$ . The reason for this is that when we later assemble the left- and right-hand-side we need it to be in integral form. Notice also that this integration holds equal to the sum as long as the domain  $\Omega$  has area 1.

Finally we compute the solution by  $LU$ -factorization.

```
A = assemble(B)
b = assemble(L)
# Computing solution
w = Function(func_space)
solve(A,w.vector(),b,'lu')
(u,U) = w.split()
```

First we assemble the bilinear form and right hand side. Next we define  $w$  to be a function defined on the function space defined earlier. Finally to get the solution  $(u, U)$  we split  $w$ .

For the second method defined in (4.3) the code looks as follows:

```
(u,U,c) = TrialFunctions(func_space)
(v,V,d) = TestFunctions(func_space)

a = (inner(sigma*grad(u),grad(v)))*dx \
+ sum([1/z[i]*(u-U[i])*(v-V[i])*ds(i) for i in range(N)]) \
      + (c*sum([V[i] for i in range(N)])*dx) \
      + (d*sum([U[i] for i in range(N)])*dx)

L = sum([I[i]*V[i]*ds(i) for i in range(N)])

A = assemble(a)
b = assemble(L)

# Computing solution
w = Function(func_space)
solve(A,w.vector(),b,'lu')
(u,U,c) = w.split()
```

Notice, that when we implement the parts  $c \sum_{k=1}^N V_k$  and  $d \sum_{k=1}^N U_k$ , we do it by  $c \int_{\Omega} \sum_{k=1}^N V_k$  and  $d \int_{\Omega} \sum_{k=1}^N U_k$ . This is again due to the assembling.

## B.4 Calculating errors

In the thesis there are different errors which need to be computed. Say we want to compute the error between the computed solution  $u_h$  and  $u$  in  $L^2(\Omega)$  and  $H^1(\Omega)$ . Then one can do this the simplest way by:

```
L2error =sqrt(assemble((u-uh)**2*dx))
H1error =sqrt(assemble((u-uh)**2*dx\
                    +inner(grad(u-uh),grad(u-uh))*dx))
```

This is the easiest and fastest way to compute the error. There are although situations where this is not a good measure of the error, since the compiler might expand by:

```
(u-uh)**2*dx = u**2*dx + uh**2*dx - 2*u*uh*dx
```

This is especially a bad thing in situations where  $u$  and  $u_h$  are close to each other. In these cases a lot of the errors will be a sum of computer uncertainties. Furthermore the number of computer uncertainties which are summed depend on the mesh. Thus a fine mesh could give a larger error than a rough mesh.

Therefore a better, but slower, method of computing the error is by the built in `errornorm`-function. This function computes the error by raising the degree of the polynomials un which  $u$  and  $u_h$  are defined. We will in general work with a degree-raise of order 3.

```
dolfin.fem.norms.errornorm(u, uh, norm_type='L2',\
                           degree_raise=3)
```

## B.5 Algorithm for the inverse problem

In this section we show how the algorithm for the inverse problem are implemented in FEnICS. In our results we always know the correct conductivity and then produce the magnitude of the current density from that. Thus we first solve the forward problem with conductivity  $\sigma$  to get the function  $u$ . Then the magnitude  $a = \sigma|\nabla u|$  are computed by:

```
a = project(sigma*sqrt(inner(gradu,gradu)),H)
```

The projection on to the space  $H$  are necessary, since we will use the current density inside the algorithm of the inverse problem. Before running the algorithm

we need to define a tolerance for when to stop. We would like this tolerance to depend on the size of  $a$ . This could either be the  $L^2$ -norm of  $a$  or the smallest value that  $a$  takes. It is described earlier how to compute the norm. To find the smallest value of  $a$ , we write  $a$  as an array containing all the values of  $a$  in the mesh points. This is done by

```
minimum = min(a.vector().array())
```

And this is also case why we need to project  $a$  onto the space. The tolerance can now be computed. We will mainly have a tolerance of 1% – 2% of the size of  $a$ . We are now ready to run the while-loop.

```
# Running while-loop
while error > tolerance:

    # Compute solution of forward problem
    (u,U) = TrialFunctions(func_space)
    (v,V) = TestFunctions(func_space)

    B = (inner(sigma*grad(u), grad(v))*dx\
          +sum([(u-U[i])*(v-V[i])*ds(i) for i in range(N-1)])\
          +((u+sum([U[i] for i in range(N-1)]))\
            *(v+sum([V[i] for i in range(N-1)])))*ds(N-1)

    L = sum([I[i]*V[i]*ds(i) for i in range(N-1)]) \
          + (I[N-1]*sum([-V[i] for i in range(N-1)]))*ds(N-1)

    A = assemble(B)
    b = assemble(L)

    w = Function(func_space)
    solve(A,w.vector(),b,'lu')
    (u,U) = w.split()

    # Computing error
    atilde = project(sigma*sqrt(inner(grad(u),grad(u))),H)
    error = sqrt(assemble((a-tilde)**2*dx))

    # Compute new conductivity
    sigma = project(a/(sqrt(inner(grad(u),grad(u))),H)
```

Here we have computed the error, by the  $L^2$ -norm of  $a - \tilde{a}$ . One could also compute it by the  $L^\infty$ -norm, i.e.

```
error_func = project(a-tilde,H)
error = max(error_func.vector().tilde())
```

We will mainly consider the error as the  $L^2$ -norm of the difference. When finished running the algorithm we have a pair  $(\tilde{\sigma}, \tilde{u})$ , which satisfies  $\tilde{\sigma}|\nabla\tilde{u}| \approx a$ . Thus we can create the  $\phi$ -function. We will although not really compute the  $\phi$ -function, but instead  $u^* = \phi(\tilde{u})$  and  $\sigma^* = (\phi'(\tilde{u}))^{-1}\tilde{\sigma}$  directly from the knowledge of  $u$  on the boundary. Assume that  $\mathbf{U}$  is a vector containing the values of  $u$  at points of the boundary and  $\mathbf{UTILDE}$  is its similar for  $\tilde{u}$ . Then we compute the final conductivity and solution of the forward problem by: First we write  $\tilde{u}$  and  $\tilde{\sigma}$  as arrays representing the values of the node points. For each node-point we find the value of  $\tilde{u}$ , and match this value with two values in  $\mathbf{UTILDE}$  as:

```
k = utilde[i]
j = 0
while k > UTILDE[j] and j < len(UTILDE):
    j = j+1
```

Now we know that  $\mathbf{UTILDE}[j-1] \leq \tilde{u}[i] \leq \mathbf{UTILDE}[j]$ . If  $j$  is neither 0 or  $\text{len}(\mathbf{UTILDE})$ , which we will handle as special cases, we compute the new values of  $\mathbf{utilde}[i]$  and  $\mathbf{sigmatilde}[i]$  by

```
a = (U[j]-U[j-1])/(UTILDE[j]-UTILDE[j-1])
utilde[i] = a*(k-UTILDE[j-1])+U[j-1]
sigmatilde[i] = 1.0/a*sigmatilde[i]
```

Notice that this corresponds to computing  $\phi'$  by (5.18). Regarding the special cases, note that these should in principle not occur since the range of  $u$  and  $\tilde{u}$  on  $\Upsilon$  should be equal to the ranges on  $\bar{\Omega}$ . But due to numerical approximations they can occur. Anyway if this occurs we extend the affine function computed in the neighbouring points, s.t. if  $j = 0$ , we compute  $\mathbf{a}$  by:

```
a = (U[1]-U[0])/(UTILDE[1]-UTILDE[0])
```

and if  $j = \text{len}(\mathbf{UTILDE})$ :

```
a = (U[-1]-U[-2])/(UTILDE[-1]-UTILDE[-2])
```

Then  $u^*$  and  $\sigma^*$  are now computed by:

```
ustar = Function(H)
ustar.vector()[:] = utilde
sigmatar = Function(H)
sigmatar.vector()[:] = sigmatilde
```

Finally  $\sigma_2^*$  is computed through the current density  $\mathbf{a}$  as:

```
sigmatar2 = a/sqrt(inner(grad(ustar), grad(ustar)))
```



# Original Project Plan

---

In this Appendix is the original project plan and learning objectives for the thesis.

## C.1 Original Project Plan

We will in this thesis consider the scenario where one attached a number of electrodes to the boundary of a domain and apply a current to each of them.

We will use the Complete Electrode Model (CEM) for EIT as a model for this scenario. Using the CEM we will consider two main problems.

The first problem we will consider is the one of finding the voltage in the interior domain as well as on the electrodes when knowing the conductivity in the interior. This problem is referred to as the forward problem. We will show that this problem under certain circumstances has a unique solution. This is done through two different approaches. Firstly we will consider the problem through a variational formulation and using Lax-Milgram we will achieve uniqueness. The second approach is by considering the problem as a minimization of a functional. Finally we use FEnICS to solve various cases numerically.

The second problem is the inverse problem of finding the conductivity in the interior. We will show how this problem does not have a unique solution and characterize this non-uniqueness. By this characterization we will also show how knowledge of the current density inside the domain and the voltage at some part of the boundary can help to solve the problem. We will solve the problem by creating an algorithm. These situation are also visualized using FEnICS.

The theory which I will go through will be for dimensions  $d = 2, 3$ . The numerical solutions will be done in two dimensions and the domain will be the unit square. Although if time allows I will consider doing numerical computations in three dimensions, by considering the unit-box as domain, or I will try with other domains in two dimensions, for example the unit circle. Furthermore, if time is there, I will consider doing some optimization of the problem.

### C.1.1 Learning objectives

The learning objectives of the thesis is:

- Understand and state the problems, models etc. within EIT and CDII.
- Be able to state, prove and understand mathematical theorems, lemmas and propositions within EIT and CDII.
- Combine and compare theorems, propositions etc.
- Obtain further knowledge within the fields of partial differential equations, functional analysis, etc..
- Learn Python programming and FEnICS for solving partial differential equations.
- Be able to solve problems within EIT and CDII numerically.

### C.1.2 Goals

#### 1. Theory of CEM and numerical solution of forward problem:

1.1: Proving that a function is a solution to the forward problem if and only if it solves a bilinear form.

1.2: Proving that there is a unique solution of the forward problem, given some conditions.

1.3: Implementing the CEM in FEnICS, solving it in the unit square domain and finding the convergence rate.

## **2. Theory of CDII:**

2.1: Proving the solution to the forward problem is a global minimizer of a functional.

2.2: Proving and characterizing non-uniqueness of the CDII problem.

2.3: Proving maximum principle for CEM and uniqueness up to a constant.

## **3. Numerical implementation of CDII:**

3.1: Designing a solver for the CDII problem.

3.2: Solving the CDII problem.

## **4. If time allows it:**

4.1: Consider the problem in three dimensions or in another domain.

4.2: Doing some kind of optimization.



# Bibliography

---

- [DL88] R. Dautray and J-L. Lions. *Mathematical Analysis and Numerical Methods for Science and Technology, Volume 2, Functional and Variational Methods*. Springer-Verlag, 1988.
- [DS15] Jeremi Darde and Stratos Stambouli. Electrode modelling: The effect of contact impedance. *ESAIM: Mathematical Modelling and Numerical Analysis*, 2015.
- [Eva10] Lawrence C. Evans. *Partial Differential Equations*. American Mathematical Society, 2010.
- [GT01] D. Gilbarg and N. S. Trudinger. *Elliptic Partial Differential Equations of Second Order*. Springer, 2001.
- [KZ05] Andrew J. Kurdila and Michael Zabaranin. *Convex Functional Analysis*. Birkhäuser, 2005.
- [LM73] J. L. Lions and E. Magenes. *Non-Homogeneous Boundary Value Problems and Applications*. Springer, 1973.
- [MS12] Jennifer L. Mueller and Samuli Siltanen. *Linear and Nonlinear Inverse Problems with Practical Applications*. SIAM, 2012.
- [NTV15] Adrian Nachman, Alexandru Tamaskan, and Johann Veras. A weighted minimum gradient problem with complete electrode model boundary conditions for conductivity imaging. 2015.
- [SCI92] Erkki Somersalo, Margaret Cheney, and David Isaacson. Existence and uniqueness for electrode models for electric current computed to-

mography. *SIAM Journal on Applied Mathematics*, 52(4):1023–1040, 1992.